Page Denied

STAT

Next 1 Page(s) In Document Denied

ELECTRICAL COMMUNICATIONS

Monthly Scientific and Technical Journal

Organ of the Ministry of Communications of the USSR

Tenth year of publication. No.4, April, 1956

TABLE OF CONTENTS

STAT

BOARD OF EDITORS

STAT

QUICKER FULFILLMENT OF THE DIRECTIVES OF THE 20th CONGRESS OF THE CPSU ON EXCHANGE OF TELEVISION PROGRAMS BETWEEN CITIES

Enormous tasks were set by the historic 20th Congress of the Communist Party of the Soviet Union before the Soviet people.

In the sixth Five-Year Plan, all branches of the national economy are to rise to a higher technical level, based on a consistent and rational incorporation of the most advanced scientific methods and equipment. Soviet scientists and engineers are successfully solving highly complex problems in technical progress. It suffices to recall the new field created around the use of atomic energy for peaceful purposes. In this branch of science, the accomplishments of Soviet scientists are so great that the sixth Five-Year Plan envisions the construction of atomic electrical stations having an over-all power of 2.5 million kilowatts. We might also recall the work done on electronic computers for solving complex mathematical problems, and many other achievements of Soviet science.

Our accomplishments in the field of electrical communications are also numerous, but we must at the same time recognize the backwardness of several branches of electrical communications. Thus, in his report to the 20th Congress of the CPSU, comrade N.S.Khrushchev stated that "...the level of development of means of communication, particularly radio relay lines, phototelegraphy and television broadcasting, still do not satisfy the needs of the population and the national economy".

In the resolutions of the 20th Congress great attention was paid to further and more rapid development of television in the Soviet Union.

The Congress directives with regard to the sixth Five-Year Plan provide that by 1960 the number of television stations will be no less than 75. Special communication channels must be created for the exchange of programs between the television stations of Moscow, Leningrad, the capitals of Union Republics, and other large cities.

STAT

0

QUICKER FULFILLMENT OF THE DIRECTIVES OF THE 20th CONGRESS OF THE CPSU ON EXCHANGE OF TELEVISION PROGRAMS BETWEEN CITIES

Enormous tasks were set by the historic 20th Congress of the Communist Party of the Soviet Union before the Soviet people.

In the sixth Five-Year Plan, all branches of the national economy are to rise to a higher technical level, based on a consistent and rational incorporation of the most advanced scientific methods and equipment. Soviet scientists and engineers are successfully solving highly complex problems in technical progress. It suffices to recall the new field created around the use of atomic energy for peaceful purposes. In this branch of science, the accomplishments of Soviet scientists are so great that the sixth Five-Year Plan envisions the construction of atomic electrical stations having an over-all power of 2.5 million kilowatts. We might also recall the work done on electronic computers for solving complex mathematical problems, and many other achievements of Soviet science.

Our accomplishments in the field of electrical communications are also numerous, but we must at the same time recognize the backwardness of several branches of electrical communications. Thus, in his report to the 20th Congress of the CPSU, comrade N.S.Khrushchev stated that "...the level of development of means of communication, particularly radio relay lines, phototelegraphy and television broadcasting, still do not satisfy the needs of the population and the national economy".

In the resolutions of the 20th Congress great attention was paid to further and more rapid development of television in the Soviet Union.

The Congress directives with regard to the sixth Five-Year Plan provide that by 1960 the number of television stations will be no less than 75. Special communication channels must be created for the exchange of programs between the television stations of Moscow, Leningrad, the capitals of Union Republics, and other large cities.

STAT

QUICKER FULFILLMENT OF THE DIRECTIVES OF THE 20^{th} CONGRESS OF THE CPSU ON EXCHANGE OF TELEVISION PROGRAMS BETWEEN CITIES

Enormous tasks were set by the historic 20^{th} Congress of the Communist Party of the Soviet Union before the Soviet people.

In the sixth Five-Year Plan, all branches of the national economy are to rise to a higher technical level, based on a consistent and rational incorporation of the most advanced scientific methods and equipment. Soviet scientists and engineers are successfully solving highly complex problems in technical progress. It suffices to recall the new field created around the use of atomic energy for peaceful purposes. In this branch of science, the accomplishments of Soviet scientists are so great that the sixth Five-Year Plan envisions the construction of atomic electrical stations having an over-all power of 2.5 million kilowatts. We might also recall the work done on electronic computers for solving complex mathematical problems, and many other achievements of Soviet science.

Our accomplishments in the field of electrical communications are also numerous, but we must at the same time recognize the backwardness of several branches of electrical communications. Thus, in his report to the 20^{th} Congress of the CPSU, comrade N.S.Khrushchev stated that "...the level of development of means of communication, particularly radio relay lines, phototelegraphy and television broadcasting, still do not satisfy the needs of the population and the national economy".

In the resolutions of the 20^{th} Congress great attention was paid to further and more rapid development of television in the Soviet Union.

The Congress directives with regard to the sixth Five-Year Plan provide that by 1960 the number of television stations will be no less than 75. Special communication channels must be created for the exchange of programs between the television stations of Moscow, Leningrad, the capitals of Union Republics, and other large cities.

This task, which has exceptional political and cultural importance, can be fulfilled by using coaxial cables and radio relay lines. We must note the slowness of our radio industry in manufacturing the necessary equipment. We might have long ago organized television exchange between Moscow and Leningrad, where coaxial cable lines were laid many years ago. Leningrad has a large technical force on whom we depend for the rapid development of equipment for video transmission over the existing coaxial cable network. We can only be surprised at the slowness of those who should have organized this work.

The decisive role in the matter of organizing intercity television channels for exchanging programs should be given to radio relay lines. The directives of the 20th Congress provide for the creation of a wide network of radio relay lines and the installation of no less than 10 thousand kilometers of these lines during the coming five-year period.

In conjunction with the resolution of the government, 1958 should see the construction of a radio relay line for television exchange between Leningrad, Tallin, Riga, Vilnius, and Minsk. Plans for radio relay lines in the southern and eastern areas have been initiated.

To realize this large program we must begin immediately to carry through a number of strict measures. First of all we must speed up the development of the radio relay equipment being worked on in the laboratories of the Ministry of Communications, and at the same time see to it that the radio engineering industry joins in this work so as to assure the most rapid organization of production on the necessary scale, beginning with 1957. This can be done only under close cooperation between the institutes and construction bureaus of the Ministry of Communications and MRTP (Ministry of the Radio Engineering Industry), which should be realized immediately.

The Congress directives make provisions for starting color television. In the last Five-Year Plan, the laboratories of the MRTP wasted a great deal of effort on designing color television with alternate transmission of colors. This system required video signal band transmission above 12 megacycles, which made it impossible to transmit color televisión over coaxial cables. Since we are not creating a color television system with simultaneous transmission of colors compatible with black-and-white television, using a frequency band of 6 mc, planning for coaxial cable and radio relay construction should take into account the transmission of color television.

Radio relay lines should not only provide for the transmission of television, but also, when necessary, of many hundreds of telephone calls. Comrade N.A.Bulganin, in his report to the 20th Congress stated that "we are planning to build, during the next Five-Year Plan, no less than 10,000 kilometers of radio relay lines which will permit us to realize up to [illegible] telephone connections simultaneously in one direction".

We must be guided by this concrete figure in constructing a system for densifying radio relay lines. The system should be designed on the basis of 600 channels for each radio-frequency trunk. In the major direction we should provide three trunks, one of them for transmission of television programs (the system should provide the possibility of increasing the number of trunks to six).

To fulfill this task we must perform a great amount of work in construction and production, and also in designing and planning. In this work we must manifest great creative activity and persistence in overcoming the technical and organizational difficulties.

Since the creation of a large network of radio relay lines is one of the most pressing problems in the field of electrical communications, the fulfillment of this task must be given strictest attention.

Also, on the pages of our journal we must carry out large-scale explanation and discussion of the main technical matters involved in fulfilling this task.

STAT

RAISING THE STABILITY OF APPARATUS FORMING ONE-BAND SIGNALS

BY

A.M.SEMYONOV AND M.V.VERZUNOV

Points involved in decreasing the influence of asymmetry of balanced modulators on the suppression values of unnecessary frequency components are discussed.

Statement of the Problem

One of the most important problems which must be solved in designing transmitters operating on one frequency sideband is the problem of stable suppression of carrier frequency and of the second side band beats.

We know of two basic methods for forming a single-sideband signal: the method of repeat balance modulation and the method of multiphase modulation (phase compensation). The first method received application in powerful radio-transmitting apparatus, whereas the method of multiphase modulation, despite its simplicity, has not yet found wide practical use because of the fact that it involves certain difficulties in assuring high norms of carrier and second sideband suppression and in creating a stable suppression under the action of destabilizing factors.

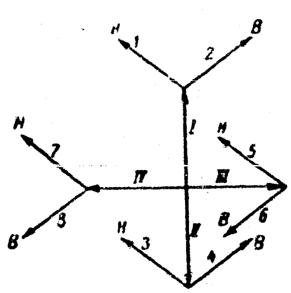

Fig.1

The most important component parts of single-band equipment, using the multiphase modulation method are a low-frequency broad-band phase converter and a multiphase modulator. The latter is (in four-phase modulation) a system of two balance modulators operating on a common load. The suppression of second sideband beats is dependent on the accuracy of the

STAT

phase shift between the voltages received from the LF and HF phase converters and the amplitude symmetry of the branch of the balanced modulators.

At present, it is possible to produce sufficiently stable broad-band phase converters ensuring the necessary phase shift with an accuracy up to 1°.

Ordinarily, when analyzing the operation of balanced modulators, it is considered that the balanced modulator is a strictly symmetric system, i.e., that the tubes and corresponding elements of the balanced modulator branches are identical, the same being true for the feeding voltages in absolute magnitude. On this basis it is concluded that the currents in the balanced modulator branches are equal in modulus.

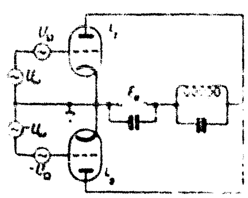

Fig.2

From an examination of the vector diagram of a four-phase modulator (Fig.1) it follows that upon complete amplitude symmetry of the balanced modulator branches, the vectors I and II, III, and IV compensate mutually, i.e., there is complete suppression of the carrier frequency; the vectors 2, [illegible], [illegible], and [illegible] also compensate one another, i.e., there is total suppression of the second sideband, whereas vectors 1,3,5, and 7 add up, giving in sum a beat of the separated frequency sideband.

However, in actual equipment of this type, special measures must be taken to obtain complete amplitude symmetry of the balanced modulator branches, to prevent residual oscillations of the carrier frequency and second sideband in the common load of the multiphase modulator.

Asymmetry in the balanced modulator may be caused by difference in the tube parameters or their change during operation, by nonidentical changes in the magnitude of the feeding foltages in the branches, by changes in the exciting and modulating voltages, and by several other factors.

Decrease in the influences of asymmetrizing factors can be obtained by using negative feedback in the balanced modulators.

The diagram of the balanced modulator is shown in Fig.2.

As we know, the amplitude of the first harmonic of the plate current is

$$I_{a_1} = SU_\omega \gamma_1(\theta). \qquad (1)$$

In linear modulation, it is

$$\gamma_1(\theta) = A_1 - a_1 \cos\theta, \qquad (2)$$

where

$$\cos\theta = -\frac{E_g + U_\Omega \cos\Omega t - E_{g*}}{U_\omega}. \qquad (3)$$

From these expressions it is not difficult to obtain an expression for the amplitude of the first harmonic of the carrier frequency current and the side frequency current.

Substituting eq.(2) into eq.(2), we get

$$\gamma_1(\theta) = A_1 + a_1\left(\frac{E_g - E_{g*}}{U_\omega} + \frac{U_\Omega}{U_\omega}\cos\Omega t\right). \qquad (4)$$

Taking eq.(4) into account and making a few simple transformations, eq.(1) will yield:

The amplitude of the carrier frequency current:

$$I_\omega = U_\omega S\left(A_1 + a_1 \frac{E_g - E_{g*}}{U_\omega}\right) \qquad (5)$$

and the amplitude of the side frequency current:

$$I_{\omega \pm \Omega} = \frac{S a_1 U_\Omega}{2}. \qquad (6)$$

The constant component of the plate current of the tube at modulation fluctuates with the audio frequency around a mean value of I_{mean} :

$$I_{a_0} = I_{mean} + I_{a\Omega} \cos \Omega t. \quad (7)$$

$$I_{mean} = SU_{\omega} \gamma_0 (\theta). \quad (8)$$

Since $\gamma_0(\theta) = A_0 - a_0 \cos \theta$, we obtain the following relation, taking eq.(3) into account:

$$I_{mean} = SU_{\omega} \left[A_0 + a_0 \frac{E_g - E_{g0}}{U_{\omega}} \right]. \quad (9)$$

$$I_{a\Omega} = a_0 S U_{\Omega}. \quad (10)$$

Examining eqs.(5) and (9), we see that

$$\frac{I_{\omega}}{I_{mean}} = \frac{S\gamma_1(\theta)}{S\gamma_0'(\theta)} = \text{const}, \quad (11)$$

where $\gamma_0' = \gamma_0$ at $U_\Omega = 0$.

Consequently, if for any reason, there is a change in the amplitude of the carrier frequency current, a change (within the same limits) will occur in the mean value of the constant component of the tube plate current.

Hence it follows that if, under the action of a destabilizing factor, the mean value of the constant component of the plate current is invariable, then [according to eq.(11)] the amplitude of the carrier-frequency current should also remain equal to its value before the action of the destabilizing factor. This problem can be solved, as shown below, by using negative feedback corresponding to the mean value of the constant component of the tube plate current.

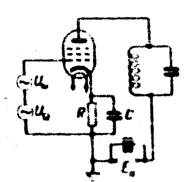

Fig.3

It follows from eq.(6) that if, on any change in transconductance, we change the amplitude of the modulating voltage accordingly, the side-frequency current will remain unchanged in amplitude.

As indicated in eq.(10), the amplitude of the modulating voltage can be influenced by the change in the audio-frequency current component of the tube plate current, i.e., negative feedback can be obtained in accordance with the audio-frequency current.

It is obvious that all above statements on the action of negative feedback in connection with the audio-frequency current, upon any change in transconductance are also valid for the case where the transconductance remains unchanged while the modulating voltage is one of the balanced modulator branches has changed.

<u>Negative Feedback in Connection with the Mean Value of the Constant Component of Plate Current</u>

In Fig.3 we show the diagram of one branch of the balanced modulator. In this diagram $\frac{1}{\Omega C} \ll R$. It is obvious that, in this case, the expression for the mean value of the constant component of the plate current will become

$$I_{mean} = SU_{\sim}\left[A_0 + a_0\frac{E_g - I_{mean}R - E_{gr}}{U_{\sim}}\right]. \qquad (12)$$

Let us suppose that under the action of some factor there is change in the grid-plate characteristic S of the tube's plate current by a magnitude εS. Then the mean value of the constant component will change by some magnitude δI_{mean}.

In this case, we will have

$$I_{mean}(1+\delta) = S(1+\varepsilon)U_{\sim}\left[A_0 + a_0\frac{E_g - I_{mean}(1+\delta)R - E_{gr}}{U_{\sim}}\right]. \qquad (13)$$

From eqs.(12) and (13) we can find an expression for δ. Dividing eq.(13) by eq.(12), we get

$$1+\delta = (1+\varepsilon)\frac{U_{\sim} + a_0E_g - a_0I_{mean}(1+\delta)R - a_0E_{gr}}{U_{\sim} + a_0E_g - a_0I_{mean}R - a_0E_{gr}}.$$

After several transformations we get

$$\zeta = \varepsilon\left[1 - a_0 \frac{I_{mean} R}{A_0 U_\omega + a_0 (E_g - E_{gv})}\right]. \qquad (14)$$

Now let us suppose that both branches of the balanced modulator have an RC feedback circuit.

In addition, we will assume that in the initial adjustment of the balanced modulator, the circuit was symmetrized in such a way that the carrier-frequency current in the common load equaled zero.

The amplitude of the first harmonic of the carrier-frequency current of each branch of the balanced modulator is

$$I_{1\omega} = I_{2\omega} = I_\omega = SU_\omega\left[A_1 + a_1 \frac{E_g - I_{mean} R - E_{gv}}{U_\omega}\right]. \qquad (15)$$

Let us also suppose that the grid-plate characteristic of one of the tubes changes by a magnitude εS; now the mean value of the plate current constant component also changes by δI_{mean}.

Then, obviously, the carrier-frequency current in this branch will have a value of

$$I'_{1\omega} = (1 + \varepsilon)\, SU_\omega\left[A_1 + a_1 \frac{E_g - I_{mean} R - I_{mean} \zeta R - E_{gv}}{U_\omega}\right], \qquad (16)$$

and the current $I_{2\omega}$ will remain constant. Since we now have $I'_{1\omega} \neq I_{2\omega}$, the load will show the difference between these currents (the remainder of the carrier-frequency current) ΔI_ω.

From eqs.(15) and (16), taking eq.(14) into consideration, we find:

$$\Delta I_\omega = \varepsilon\left\{SU_\omega\left[A_1 + a_1 \frac{E_g - I_{mean} R - E_{gv}}{U_\omega}\right] - S a_1 I_{mean} R\left[\frac{A_0 U_\omega + a_0 (E_g - I_{mean} R - E_{gv})}{A_0 U_\omega + a_0 (E_g - E_{gv})}\right]\right\}. \qquad (17)$$

The relative increment in the carrier-frequency's remainder is:

$$\delta' = \frac{\Delta I_{\omega}}{I_{\omega}} = 2\left|1 - a_1 \frac{I_0}{I_1}\left[\Delta U_{\omega} - \frac{I_{mm} R}{a_0 (E_g - \ldots)}\right]\right|. \qquad (18)$$

As can be seen from eq.(18), by means of proper choice of the resistance R of the feedback we can to a considerable extent decrease the influence of asymmetry in the balanced modulator branches on the value of the carrier frequency's remainder.

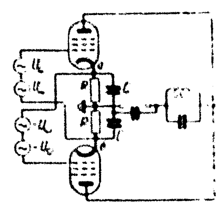

Fig..

The choice of R is only limited by the source of plate voltage.

Let us now examine the diagram presented in Fig... In contrast to the diagram with separate feedback in each branch of the balanced modulator we have here the automatic action of the result of condition change in one branch on the operating conditions of both branches. Indeed, under complete symmetry of the circuit, the voltage of the constant component of the plate current between points a and b equals zero. The change in current of one of the tubes produces a voltage between these points. This voltage changes the bias on the control grid of tubes L_1 and L_2. For example, if the current of the first tube is increased, the bias voltage on the grid of this tube increases in modulus, while it decreases on the grid of the second tube. This results in the fact that the difference in currents in the common load is decreased to a greater extent than in the previous circuit.

Let us find an expression for the remainder of the carrier-frequency current. First we will determine the value of δ.

In a symmetrical circuit, the mean value of the plate current constant component is

$$I_{mm} = S[\Delta U_m + a_0 (E_g - \ldots)]. \qquad (19)$$

On increasing the grid-plate characteristic of the plate current of the first tube by a magnitude εS, the plate current constant component of this tube increases by a magnitude δI_{mean}.

The new magnitude of the mean value of the constant component then is

$$I_{mean}(1+\delta) = (1+\varepsilon) S[A_0 U_{\sim} + a_0(E_g - \delta I_{mean} R - E_{g0})]. \qquad (20)$$

Dividing eq.(20) by eq.(19) and making simple transformations, we get

$$\delta = \frac{\varepsilon}{1 + a_0 \frac{I_{mean} R}{U_{\sim}\gamma_0(\theta)}} \qquad (21)$$

Taking the peculiarities of the given circuit into consideration, the expression for the amplitude of the first harmonic of the plate current of each tube in the absence of modulation becomes

$$I_{\sim} = S[A_1 U_{\sim} + a_1(E_g - E_{g0})]. \qquad (22)$$

When we change (e.g., increase) the grid-plate characteristic of the plate current of the first tube by a magnitude εS, the first harmonic of the plate current of the first tube changes to a value of:

$$I'_{1\sim} = (1+\varepsilon) S[A_1 U_{\sim} + a_1(E_g - \delta I_{mean} R - E_{g0})]. \qquad (23)$$

and the second tube to a value of:

$$I'_{2\sim} = S[A_1 U_{\sim} + a_1(E_g + \delta I_{mean} R - E_{g0})]. \qquad (24)$$

Using eqs.(21),(22),(23), and (24), we get an expression for the relative change in the remainder of the carrier-frequency current:

$$\xi = \frac{\Delta I_{\sim}}{I_{\sim}} = \varepsilon\left[1 - \frac{2a_1\gamma_0 RS}{\gamma_1(1 + a_0 RS)}\right].$$

STAT

where

$$\gamma_0' = A_0 + \frac{a_0}{U_m}(E_g - E_{g0}),$$

$$\gamma_1' = A_1 + \frac{a_1}{U_m}(E_g - E_{g1}).$$

A comparison of eqs.(25) and (18) shows that, in the given circuit, the effectiveness of the negative feedback is approximately twice as high as in the circuit with separate compensation for the influence of asymmetry.

Negative Feedback in Connection with the Audio-Frequency Current in each Branch of the Balanced Modulator

At complete symmetry of the multiphase modulator circuit and fulfillment of the necessary phase correlations of the modulating and exciting voltages in the common load of the modulator, oscillations of only one of the sidebands occur. As pointed out above, an asymmetry in the branch of the balanced modulator results in the appearance of oscillations of the second frequency sideband, whose amplitude is of the same order as the amplitude of the asymmetrizing factor. The introduction of negative feedback in connection with the audio-frequency current might weaken the influence of asymmetry. The diagram of one branch of a balanced modulator with negative feedback relative to the audio-frequency has the same form as the diagram given in Fig.3.

However, to realize negative feedback relative to the audio-frequency, the condition $\frac{1}{\Omega C} >> R$ must be satisfied.

In analyzing the operation of the circuit, we will limit ourselves to the simple case where the modulation is realized by the voltage of one frequency.

As shown above, the amplitude of the currents of the side frequencies is determined by eq.(6), and the component of the audio-frequency current by eq.(10). Let us suppose that, in one of the branches of the balanced modulator, the grid-plate characteristic of the tube changes by a magnitude εS. Then, the amplitude of the component of the audio-frequency current will receive an increment proportional to the increment in the grid-plate characteristic, and will have the value

$$I'_{a\Omega} = a_0 S(1+\epsilon)U_\Omega. \qquad (26)$$

As a result, an additional audio-frequency voltage will be generated at the resistance R:

$$\Delta U_\Omega = \Delta I_{a\Omega} R = a_0 S \epsilon U_\Omega R. \qquad (27)$$

Consequently, the amplitude of the modulating voltage on the tube grid will decrease by this magnitude and become equal to

$$U'_\Omega = U_\Omega(1 - \epsilon S a_0 R).$$

The new value of the side-frequency current then is

$$I'_{\omega+\Omega} = a_1(1+\epsilon)U_\Omega(1 - a_0 S\epsilon R) \qquad (28)$$

If the successive order of the phases of modulating and exciting voltages is so selected that an oscillation of the upper side frequency must be separated, then a residual voltage of the lower side frequency appears in the common load of the four-phase modulator under asymmetry.

In the absence of feedback, this residual voltage will have a magnitude of the order of ϵ:

$$\Delta I_{\omega-\Omega} = \epsilon \frac{a_1 S U_\Omega}{2} \qquad (29)$$

In the presence of feedback, the residual voltage of the low side frequency, can be reduced at will by proper selection of the parameters of the feedback circuit.

In fact,

$$\Delta I'_{\omega-\Omega} = I'_{\omega+\Omega} - I_{\omega+\Omega} = \frac{a_1 S(1+\epsilon)U_\Omega(1 - a_0 S\epsilon R)}{2} - \frac{a_1 S U_\Omega}{2} - a_1 S U_\Omega \qquad (30)$$

STAT

Here $I'_{1(\omega-\Omega)}$ and $I_{2(\omega-\Omega)}$ are the amplitudes of the currents of the lower side frequency of the first and second balanced modulators, respectively, while the prime indicates the fact that the amplitude symmetry in the balanced modulator is canceled.

Performing the obvious transformations in eq.(30) and neglecting magnitudes of the order of ε^2, we get

$$\Delta I' \; [illegible] \; \frac{1}{2}(1 \; [illegible] \; a_0SR \, a_0SU \; [illegible] \qquad (31)$$

Thus, the introduction of negative feedback corresponding to the audio-frequency current in each branch of the balanced modulators weakens the residual second side-frequency oscillation (due to amplitude asymmetry) $\frac{1}{1-a_0SR}$ times.

The resistance R is selected in accordance with the condition $R \ll \frac{1}{a_0 S}$.

Let us now examine the diagram shown in Fig.4, on the condition that $\frac{1}{\Omega C} >> R$. For any instant of time, the modulating voltages acting on the tube grids are equal to

$$U_1 \; [illegible] \; U \; [illegible] - U \; [illegible]$$
$$U_2 \; [illegible] \; U \; [illegible] + U \; [illegible]$$

Here, obviously,

$$U_1 \; [illegible] \; U_2 \; [illegible] \qquad (32)$$

Since, at complete symmetry of the circuit, a voltage drop changes the potentials of the grids relative to the audio-frequency in such a way that condition (32) is always satisfied, then this drop can be disregarded in analyzing the circuit. This voltage should be taken into consideration only when determining the numerical value of the amplitude of the modulating voltage. In the case in question, we are only interested in the change in voltage U under asymmetry of the branch of the balanced modulator.

As before, we will suppose that the grid-plate characteristic of the plate

Declassified in Part - Sanitized Copy Approved for Release 2012/10/31 : CIA-RDP81-01043R001300170001-4

current of the tube L_1 changed by a magnitude εS.

The component of the audio-frequency current of this tube will change to a value of

$$I'_{a2} = (1+\varepsilon)a_0SU_{12}.$$

Hence,

$$\Delta I_{a2} = \varepsilon a_0SU_{12}.$$

As a result of this, an additional audio-frequency voltage will appear between the points a, b:

$$\Delta U = \Delta I_{a2}R = \varepsilon a_0SU_{12}R.$$

Here the audio-frequency voltage on the grids of the tubes L_1 and L_2 will have the values

$$U'_{12} = U_{12} - \Delta U$$

and

$$U'_{22} = -U_{12} + \Delta U$$

respectively.

Until interruption of symmetry occurred, the amplitude of the current of the lower side frequency in the load of the balanced modulator had been

$$I_{(\omega-\Omega)} = \frac{a_1SU_{12}}{2} + \frac{a_1SU_{22}}{2}.$$

At asymmetry and under conditions of an open feedback loop, the current of the lower side frequency changed to a value of

$$I'_{(\omega-\Omega)} = \frac{a_1S(1+\varepsilon)U_{12}}{2} + \frac{a_1SU_{22}}{2}.$$

The residual current of the lower side frequency in the common load of a four-phase modulator in this case would have a magnitude of

$$\Delta I_{(\omega-\Omega)} = \frac{\varepsilon}{2} a_1SU_{12},$$

i.e., would be of the same order as ε.

Under conditions of a closed feedback loop, the current of the lower side fre-

Declassified in Part - Sanitized Copy Approved for Release 2012/10/31 : CIA-RDP81-01043R001300170001-4

quency in the common load from the balanced modulator, in which the symmetry is canceled, will have a value of

$$I''_{1(\omega-\Omega)} - I''_{2(\omega-\Omega)} = I''_{(\omega-\Omega)} = \frac{a_1 S(1+\varepsilon)U_\Omega(1-a_0 SR)}{2} + \frac{a_1 S U_\Omega(1-a_0 SR)}{2}.$$

In the given expression, subscripts 1 and 2 in U_Ω are omitted since $|U_{1\Omega}| = |U_{2\Omega}|$. In this case the residual current of the lower side frequency in the common load of the four-phase modulator is

$$\Delta I_{(\omega-\Omega)} = \varepsilon\left(\frac{1}{2} - a_0 SR\right)a_1 S U_\Omega.$$

Thus, the introduction of negative feedback relative to the audio-frequency current in this diagram weakens the residual current of the side frequency, produced by asymmetry, the following number of times:

$$\frac{1}{1 - 2a_0 SR} \; sep \qquad (33)$$

The resistance R is selected in accordance with the condition $R \leq \frac{1}{2a_0 S}$.

Thus, for the same feedback circuit parameters, the residual current of the second side frequency in the latter circuit is two times smaller than in the circuit with separate feedback in each branch of the balanced modulator.

Experimental Results

The aim of the experiment was to verify the validity of the above considerations and to make a quantitative determination of the gain suppressing the oscillations of the carrier frequency and second side frequency, by the use of negative feedback at asymmetry in the balanced modulator circuit. For this purpose, we constructed a model corresponding to the diagram in Fig.5. In this circuit, we applied negative feedback according to the mean value of the constant component of plate current (elements $R_1R_2R_3C_1C_2C_3$) and negative audio-frequency current feedback (elements R_3C_3).

To show the effectiveness of feedback, asymmetry of the balanced modulator branches was created artificially, by changing the voltage on the screen grid of one of the tubes. The measurements were made by means of a panorama device. The results are given in Figs.6,7 and 8. A comparison of the curves (Fig.6) shows that negative audio-frequency feedback is a highly effective means for compensating the influence of asymmetry in the branches of the balanced modulator on the amplitudes of the side-frequency current.

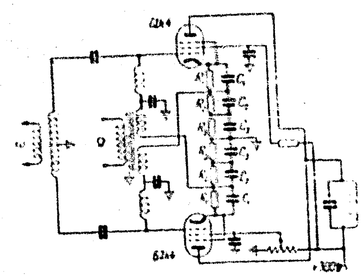

Fig.5

An examination of the graphs in Fig.7 gives interesting results. These graphs, which were calculated from experimental data, were constructed as follows: The magnitude of suppression of the second side frequency was plotted on the ordinate in decibels, and the ratio of voltages on the screen grids of the balanced modulator tubes was plotted on the abscissa. It is supposed that, at initial adjustment, both balanced modulators of the four-phase system were completely symmetric. In this case, the current of the second side frequency in the common load equals zero, i.e., the suppression of the second side frequency is $N = \infty$. On cancellation of symmetry in one of the balanced modulators, a residual side frequency is generated in the common load, whose suppression is plotted as a function of the degree of asymmetry.

A comparison of the curves shows that, for an asymmetry of 10-20% (the most probable case), the use of negative feedback gives a gain in suppression of the second frequency sideband of 15-25 db.

In the experiment, we studied the influence of negative feedback on the amplitude stability of the residual carrier frequency voltage at any change in the degree of the asymmetrizing factor. The influence of the negative feedback was estimated under the following conditions: At connected resistor of the feedback circuit

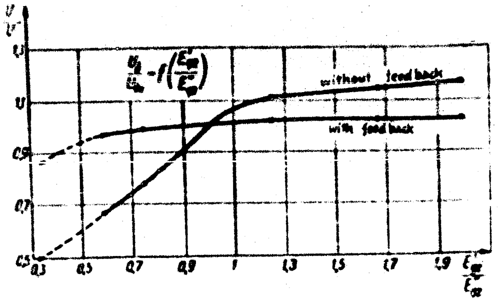

Fig.6

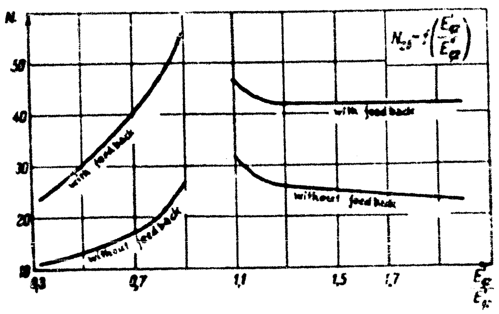

Fig.7

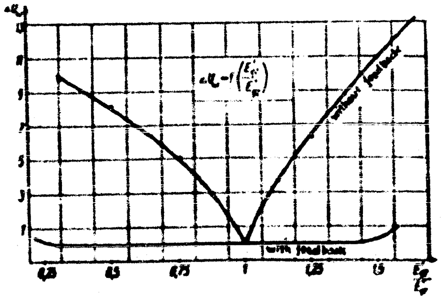

Fig.8

Declassified in Part - Sanitized Copy Approved for Release 2012/10/31 : CIA-RDP81-01043R001300170001-4

(R_1, R_2, and R_3), only the voltage of the carrier-frequency ($U_\Omega = 0$) was applied to the grids of L_1 and L_2. The residual carrier-frequency voltage was measured by a vacuum-tube voltmeter, connected to the output circuit of the balanced modulator. At equal voltages on the screen grids of the tubes, the bias voltage on the control grids was measured. This yielded the relation $\Delta U_\omega = f\left(\frac{E'_{g2}}{E''_{g2}}\right)$. After this, the resistors R_1, R_2, and R_3 were short-circuited, and the control grids of the tubes were supplied with negative bias from a source of constant voltage having the same value as with the resistors connected; this gave the relation $\Delta U = f' \frac{(E'_{g2})}{E''_{g2}}$ (without feedback). The results of the measurements are given in Fig.8. The resultant curves clearly show the effectiveness of negative feedback.

In addition, the tubes in one of the branches of the balanced modulator were replaced. We took, at random, five 6Zh4 and three 6P9 tubes.

The voltage of the side frequency was measured with audio-frequency feedback and without. At initial adjustment, the side-frequency voltage with feedback was established as 35 volts. The results of the experiment are given in Table 1.

Table 1

Type of tube	6Zh4	6Zh4	6Zh4	6Zh4	6Zh4	6P4	6P4	6P4
U_{side} with feedback, in volts	35	35	35	35	35	34	34	35.5
U_{side} without feedback, in volts	36	37	36	34	36	40	40	39

On introducing negative audio-frequency feedback it is natural to expect some decrease in the modulation depth in each branch of the balanced modulator. Considering that, without feedback, $m = \frac{U_\Omega}{U_\omega}$, then the modulation index, with feedback, decreases by a magnitude $\Delta m = \frac{\Delta U_\Omega}{U_\omega}$; this had actually been observed in the experiment. However, the decrease in modulation depth can always be compensated by a corresponding change in the modulating voltage.

It is of interest to estimate the change in modulation depth for different frequencies of the modulating voltage. However, the small value of the resistance R_3 in the feedback circuit in comparison with the value of the capacitative resistance of the blocking capacitor guarantees an insignificant change in the feedback voltage on any change in the frequency of the modulating voltage.

Thus, where R_3 = 1000 ohms and C_3 = 1000 μμf, the change in the modulation depth (with regard to its value at the mean modulating frequency of 1000 cps) is 0.5% at a frequency of 300 cps and 2.2% at 3000 cps.

Hence the circuit described above does not require special corrections in the feedback circuit to maintain a constant modulation index.

Conclusions

The above-described methods for raising the operational stability of balanced modulators used in single-band radio communications permit greater use of the multiphase modulation method in the formation of single-band signals.

In addition, negative feedback is also useful in other equipment containing balanced modulators where a constant level of output voltages is required.

BIBLIOGRAPHY

1. Bode, G. - Theory of Circuits and Designing Amplifiers with Feedback. GIIL, (1948)
2. Aseyev, B.P. - Phase Correlations in Radio Engineering, Svyaz'izdat (1954)

Article received by the Editors on 5 January, 1954

STAT

237

HARMONIC ANALYSIS OF ASYMMETRICAL PULSES*

BY

S.I.EVTYANOV

Formulas for calculating the harmonics of asymmetric pulses of plate current, obtained with a vacuum-tube oscillator operating on a complex load, are presented.

Introduction

Recently a number of articles devoted to the operation of a vacuum-tube oscillator on a complex load were published (Bibl.1-3). It was found that an overvoltage oscillator under complex load possesses a number of properties that are of considerable practical interest. The fundamental peculiarity of the system under complex load lies in the fact that the plate current pulses are asymmetric. To construct a theory for such systems we must create a simple mathematical scheme for harmonic analysis of asymmetric pulses.

The first report on operation of an oscillator at complex load and on construction of the corresponding load characteristics was the dissertation by M.G.Margolin (Bibl.4). The formulas obtained in this study for the harmonic analysis of asymmetric pulses are very cumbersome; no simple rules for constructing mathematical formulas are given.

In addition, the harmonic analysis of asymmetric pulses was studied by Z.I.Model and others (Bibl.5). In this article, the asymmetry of the pulses was obtained from the complex load for the third harmonic. This article is of considerable interest since it takes into account the influence of the third harmonic on the

---

* Submitted on 15 March 1956 to the Transmitter Equipment Meeting of the A.S.Popov Scientific Society of Radio Engineering and Electric Communication.

248

shape of the pulse; however, here too, no simple formulas for the harmonic analysis of asymmetric pulses are given.

The harmonic analysis of asymmetric pulses was also discussed by S.A.Drobov (Bibl.6). He constructed load characteristics covering a considerable range of variation in the utilization factor of the plate voltage (ξ), but calculation is only given for $\xi < 1$. No mathematical formulas for $\xi > 1$ are developed.

The aim of the present article is to establish certain rules which might yield formulas for the harmonics of asymmetric pulses in approximately the same way as this is done now for symmetric pulses.

It is presupposed that the voltages on the grid and plate of the tube are sinusoidal, i.e., the upper harmonics of the voltages are disregarded.

Approximation of Static Characteristics

To describe the static characteristics of the plate current of a triode oscillator we will approximate them with line segments. In the region where the grid current is low, the plate current is described by the expression for the emission current:

$$i = S[e_c - E_c' + D(e_a - E_a)]. \qquad (1)$$

Here e_c and e_a are the instantaneous voltages on the grid and plate; E_c' is the cutoff voltage on the grid at the operating plate voltage E_a. The remaining symbols need no special explanation.

In the region where the grid current has a considerable magnitude, the plate current in coordinates i_a, e_a is represented by a straight line passing through the coordinate origin and having a slope S_k:

$$i_a = S_k e_a. \qquad (2)$$

This line is called the critical line. A comparison of eqs.(1) and (2) gives an expression for the slope of the critical line:

$$S_k = S\left(\frac{1}{\varkappa} + D\right). \qquad (3)$$

STAT

The coefficient $\varkappa$ determines the correlation of voltages on the boundary of the region corresponding to the incipient increase in grid current

$$e_a = \varkappa(e_c - E'_c - DE_a). \tag{4}$$

The grid current can be defined as the difference between the emission and plate currents

$$i_c = i - i_a. \tag{5}$$

After substituting eqs.(1) and (2) into eq.(5) while taking account of eq.(3), we get an expression describing the characteristics of the grid current:

$$i_c = S\left(e_c - E'_c - DE_a - \frac{1}{\varkappa} e_a\right). \tag{6}$$

It is evident that these expressions are not valid at all voltages. Equation (3) is valid if $i > 0$, just as eq.(2) is valid if $i_a > 0$ and, in addition, if $i_a < i$. Corresponding limitations also apply to eq.(6).

It is essential to emphasize that if we accept the validity of the critical-line eq.(2) for tetrodes and pentodes, we will find that all the other equations also are valid. It is only necessary that the cutoff voltage E'_c be defined for the operating voltages on the screen and suppressor grids*. Here the grid current means the total current of the grids, which is close to the current of the screen grid.

Correlation of Phases with the Oscillator Operating on Complex Load

When the oscillator is operating on a complex load, the phases of the voltages on the grid and load do not coincide. Therefore, for the instantaneous voltages on the grid and plate we can write the following expressions:

$$e_c = E_c + U_c \cos(\tau - \varphi), \tag{7}$$

$$e_a = E_a - U_a \cos\tau. \tag{8}$$

* It is assumed that the voltage on the suppressor grid is $E_{cz} \geq 0$.

STAT

To construct the pulse of the emission current we must substitute eqs.(7) and (8) into eq.(1). After transformations, we get

$$i = S[E_c - E'_c + U\cos(\tau - \psi)]. \qquad (9)$$

Here U is the amplitude of the control voltage, and ψ the phase difference of the control voltage and the voltage on the load. To determine U and ψ it is convenient to make use of the vector diagram presented in Fig.1. In vector form, the complex amplitude of the control voltage is determined by the formula:

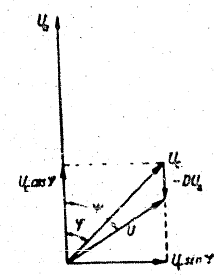

Fig.1

$$U = U_c - DU_a.$$

It follows from the diagram that the amplitude of U is determined by the expression:

$$U = \sqrt{(U_c\cos\varphi - DU_a)^2 + (U_c\sin\varphi)^2},$$

which, after simplification, will read

$$U = \sqrt{U_c^2 + (DU_a)^2 - 2U_c DU_a\cos\varphi}. \qquad (10)$$

The phase difference of the voltage on the load and the control voltage is determined by the expression:

$$\mathrm{tg}\,\psi = \frac{U_c\sin\varphi}{U_c\cos\varphi - DU_a}. \qquad (11)$$

Assuming in eq.(9) that i = 0, where $\tau - \psi = \pm\theta$, we obtain an expression for the cutoff angle of the emission current:

$$\cos\theta = -\frac{E_c - E'_c}{U}. \qquad (12)$$

In an analogous way, after substituting eqs.(7) and (8) into eq.(6), we can obtain an expression for the grid current:

$$i_c = S\left[E_c - E'_c - \left(D + \frac{1}{\kappa}\right)E_a + U_1\cos(\tau - \varphi_1)\right]. \qquad (13)$$

Here the amplitude of the control voltage for the grid current is:

$$U_1 = \sqrt{U_c^2 + \left(\frac{1}{\kappa}U_a\right)^2 + 2U_c\frac{1}{\kappa}U_a\cos\varphi}. \qquad (14)$$

The phase difference of the control voltage for the grid current and the voltage on the load is as follows:

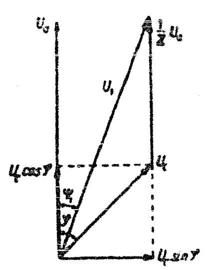

Fig.2

$$\operatorname{tg}\varphi_1 = \frac{U_c\sin\varphi}{U_c\cos\varphi + \frac{1}{\kappa}U_a}. \qquad (15)$$

Equations (14) and (15) differ from eqs.(10) and (11) by the substitution of $-(1/\kappa)$ for D. The vector diagram in Fig.2 serves to explain the calculation of the amplitude and phase of the control voltage for the grid current.

Assuming in eq.(13) that $i_c = 0$, where $\tau - \varphi_1 = \pm\theta_1$, we obtain an expression for the cutoff angle of the grid current:

$$\cos\theta_1 = -\frac{E_c - E'_c - \left(D + \frac{1}{\kappa}\right)E_a}{U_1}. \qquad (16)$$

Formation of Plate Current Pulse

When the oscillator is operating on a complex load, the construction of the plate current pulses by means of dynamic characteristics is inconvenient, since portions of the dynamic characteristics are formed of segments of an ellipse. The most advisable procedure is to construct the pulse as segments of corresponding sinusoids, as shown in Fig.3. In this diagram, we plotted the emission current pulse from eq.(9), and the plate current graph from an equation obtained from eq.(2) after substituting eq.(8):

$$i_a = S_k(E_a - U_a \cos\tau). \qquad (17)$$

As long as $i < i_a$, the plate current is determined by a segment of a sinusoid with the amplitude SU, constructed on the level $S(E_c - E_c')$. If, on the other hand, $i_a < i$, the plate current is determined by the ordinates of an inverted sinusoid with the amplitude $S_k U_a$, constructed on the level $S_k E_a$. In Fig.3 we present the plate current pulse for the case of $\xi = \frac{U_a}{E_a} < 1$. Here we get an asymmetric pulse with an incomplete dip. In Fig.3 we show the phase angle and cutoff angles determined from the above formulas.

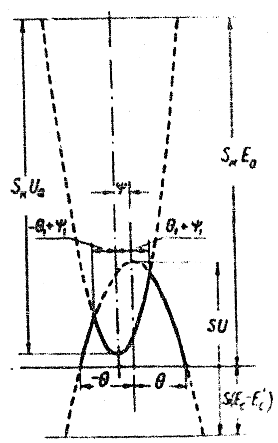

Fig.3

In Fig.4 we show the formation of a plate current pulse where $\xi > 1$. Here complete dip of the plate current occurs. As long as the plate voltage is negative, $i_a = 0$. The cutoff angle θ_2 can be determined from eq.(17) if we assume that $i_a = 0$ where $\tau = \pm\theta_2$:

$$\cos\theta_2 = \frac{E_a}{U_a} = \frac{1}{\xi}. \qquad (18)$$

In Fig.5 we show the formation of a plate current pulse at large phase angles ψ (i.e., with highly disturbed load) and considerable magnitude of ξ. This case differs from that presented in Fig.4 in that the plate current pulse preserves one portion (in this case, the right part). The question arises: How are we to know, analytically, without constructing the shape of the pulse, whether it has two parts, as in

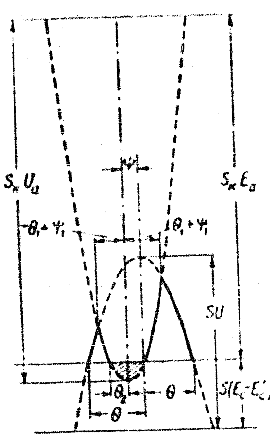

Fig.4

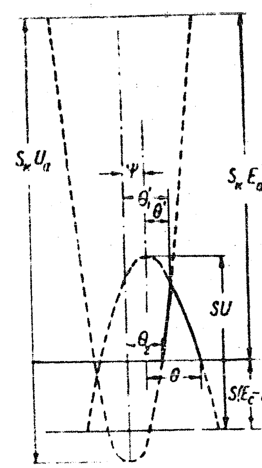

Fig.5

Fig.5? A comparison of Figs.4 and 5 shows that, for the pulse in Fig.5, the following inequation should be satisfied:

$$0 < \psi + \theta_1 - \psi_1.$$

Our problem is now to find simple formulas for determining the harmonic components of the pulses presented in Figs.3,4, and 5.

Elementary Pulses

In the harmonic analysis of complex symmetric plate current pulses, no new calculation formulas are required. We know that every symmetric complex pulse can be presented as the sum or difference of elementary pulses, for which tabulated coefficients are in existence. For symmetric pulses, the elementary pulses are the symmetric cosinusoidal pulse and the symmetric rectangular pulse. For a harmonic analysis of asymmetric pulses, the elementary symmetric pulses are unsuitable. To analyze asymmetric pulses, the asymmetric elementary pulses can be used for constructing any given complex asymmetric pulse. We find that such elementary asymmetric pulses are half of the cosinusoidal pulse presented in Fig.6, and half of the rectangular pulse presented in Fig.7. We note that these elementary pulses are also suitable for a harmonic analysis of symmetric pulses, so that they should actually be used as the basis for a harmonic analysis of both symmetric and asymmetric pulses. Attention should be paid to the fact that, for the cosinusoidal pulse (Fig.6), the amplitude of the generating cosinusoid is used as the unit, i.e., the amplitudes of the harmonics are related to the amplitude of the generating cosinusoid. For the rectangular pulse (Fig.7), its height is used as the unit, i.e., the amplitudes of the harmonics are related to the height of the pulse. We propose that $\tau = 0$ corresponds to the ordinate.

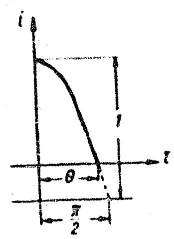

Fig.6

For the pulse in Fig.6, expansion into a Fourier series will yield

$$i = \frac{\gamma_0(\theta)}{2} + \sum_{n=1}^{\infty} \frac{\gamma_n(\theta)}{2} \cos n\tau + \sum_{n=1}^{\infty} \gamma_{ns}(\theta) \sin n\tau. \qquad (19)$$

It is essential to emphasize that, due to asymmetry of the pulse, the Fourier series contains not only even terms relative to τ, with $\cos n\tau$, but also odd terms with $\sin n\tau$. Since the amplitudes of the harmonics at $\cos n\tau$ and also the constant component in this case are equal to half the components of the symmetric pulse for which Tables have been compiled (Bibl.7), the corresponding coefficients in series (19) are divided by 2. We will call the components $\gamma_n(\theta)/2$ cophasal,

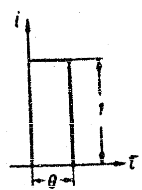

Fig.7

and the components $\gamma_{ns}(\theta)$ quadrature, since the phases of the latter lag with respect to the former by $\pi/2$. The resolution ratio of the quadrature components is determined by the expression:

$$\gamma_{ns}(\theta) = \frac{1}{\pi}\int_0^\theta (\cos\tau - \cos\theta)\sin n\tau\, d\tau.$$

For the first harmonic ($n = 1$), the computations give

$$\gamma_{1s}(\theta) = \frac{1}{2\pi}(1 - \cos\theta)^2. \qquad (20)$$

For the other harmonics, $n = 2,3\ldots$ we can obtain the expression

$$\gamma_{ns}(\theta) = \frac{1}{\pi}\left[\frac{\cos(n+1)\theta}{2n(n+1)} - \frac{\cos(n-1)\theta}{2n(n-1)} - \frac{\cos\theta}{n} + \frac{n}{n^2-1}\right]. \qquad (21)$$

The Fourier series for the pulse in Fig.7 can be written in a manner analogous to eq.(19):

$$i = \frac{\alpha_0(\theta)}{2} + \sum_{n=1}^{\infty}\frac{\alpha_n(\theta)}{2}\cos n\tau + \sum_{n=1}^{\infty}\alpha_{ns}(\theta)\sin n\tau. \qquad (22)$$

Here α_0 and α_n are the constant component and amplitudes of the harmonics of a symmetric rectangular pulse:

$$\alpha_0(\theta) = \frac{\theta}{\pi}. \qquad (23)$$

$$\alpha_n(\theta) = \frac{2}{\pi n}\sin n\theta. \qquad (24)$$

The amplitudes of the quadrature components are determined by the expression:

$$\alpha_{ns}(\theta) = \frac{1}{\pi}\int_0^\theta \sin n\tau\, d\tau.$$

After computation, we get:

$$\alpha_{ns}(\theta) = \frac{1}{\pi n}(1 - \cos n\theta). \qquad (25)$$

It is essential to emphasize that if we write out a series analogous to eqs.(19) and (22) for pulses similar to those in Figs.6 and 7 but located at the left of the ordinate, the cophasal components will remain unchanged, whereas the sign of the quadrature components will change. This fact must be taken into consideration in constructing expressions for the amplitudes of the harmonics of asymmetric pulses. This rule can easily be understood from the case of calculating a pulse of the shape presented in Fig.6, but symmetric. For this kind of pulse, the cophasal components of the harmonics will double, while the quadrature components compensate each other. It is advisable to correlate the positive cutoff angle to the right half of the pulse and the negative cutoff angle to the left half. Here we must still take into account that the cophasal coefficients are odd functions of the cutoff angle, while the quadrature coefficients are even functions.

Determining the Harmonics of Asymmetric Pulses

Let us turn to determining the harmonic components of the pulse presented in Fig.3. We might resort to the above method of resolving the complex pulse into a sum of elementary pulses and of determining the harmonic components of the complex pulse as the sum of the harmonic components of the elementary pulses. However, experience has shown that for a pulse of the type in Fig.3, this method leads to a cumbersome expression which can only be simplified after complicated transformations. Therefore, for the pulse in Fig.3 it is advisable to apply another technique. Where $\xi < 1$, the grid current pulse is a symmetric cosinusoidal pulse, and therefore it is simplest to define the harmonic components of the plate current pulse as the difference between the harmonic components of the emission and grid currents. Thus, for the constant component of the plate current we get the expression:

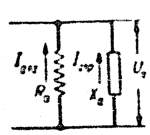

Fig.8

$$I_{a0} = SU\gamma_0(\theta) - SU_1\gamma_0(\theta_1). \qquad (26)$$

STAT

Here U and θ, U_1 and θ_1 are determined by eqs.(10), (12), (14), and (16), respectively.

In determining the components of the first plate-current harmonic, it is advisable to start counting off the phases with the phase of the voltage on the load. Then the current component, cophasal with the voltage, will be an active current component, and the quadrature current component will be a reactive component which has a phase lag, relative to the active component, of $\pi/2$. We will denote the amplitude of the first harmonic of the active component by I_{a1a}, and the amplitude of the first harmonic of the reactive component by I_{a1p}. In this kind of determination of the current components it is simple to find the active and reactive conductances of the load by means of a parallel equivalent circuit as shown in Fig.8:

$$\frac{1}{R_a} = \frac{I_{a1a}}{U_a},$$

$$\frac{1}{X_a} = \frac{I_{a1p}}{U_a}.$$

In determining the plate-current components we must bear in mind that the phases of the first harmonics of the emission and grid currents coincide with the phases of the corresponding control voltages. Thus, taking the phase correlations into account in the vector diagrams of Figs.1 and 2, we obtain the following expressions for the active and reactive components of the plate current:

$$\left.\begin{aligned} I_{a1a} &= SU\cos\psi\gamma_1(\theta) - SU_1\cos\psi_1\gamma_1(\theta_1) \\ I_{a1p} &= SU\sin\psi\gamma_1(\theta) - SU_1\sin\psi_1\gamma_1(\theta_1) \end{aligned}\right\}. \quad (27)$$

These expressions can be simplified if we note from the vector diagrams in Figs.1 and 2 that the following identities are valid:

$$\left.\begin{aligned} U\cos\psi &= U_c\cos\varphi - DU_a \\ U\sin\psi &= U_c\sin\varphi \end{aligned}\right\} \quad (28)$$

$$\left.\begin{aligned} U_1 \cos \psi_1 &= U_c \cos \varphi + \frac{1}{\varkappa} U_a \\ U_1 \sin \psi_1 &= U_c \sin \varphi \end{aligned}\right\} \qquad (28)$$

Therefore, eq.(27) can be rewritten as follows:

$$I_{a1a} = S(U_c \cos \varphi - DU_a)[\gamma_1(\theta) - \gamma_1(\theta_1)] - S_k U_a \gamma_1(\theta_1). \qquad (29)$$

$$I_{a1p} = SU_c \sin \varphi [\gamma_1(\theta) - \gamma_1(\theta_1)]. \qquad (30)$$

In eq.(2), S_k is the slope of the critical line in terms of eq.(3).

Equations (29) and (30) are characterized by simplicity and clarity. They include only the assigned voltages U_c, U_a, and their phase difference. If we assume that $\varphi = 0$, we obtain a formula for the amplitude of the first harmonic of a symmetric pulse. The validity of this formula is substantiated in Fig.3.

For the upper harmonics we obtain formulas analogous to eq.(27):

$$\left.\begin{aligned} I_{ana} &= SU \cos n\psi \gamma_n(\theta) - SU_1 \cos n\psi_1 \gamma_n(\theta_1) \\ I_{anp} &= SU \sin n\psi \gamma_n(\theta) - SU_1 \sin n\psi_1 \gamma_n(\theta_1) \end{aligned}\right\} \qquad (31)$$

Let us now determine the harmonics of the pulse in Fig.4. The harmonic components of this pulse can best be determined by making use of the formulas obtained for the pulse in Fig.3, and by introducing a correction to take account of the error caused by the pulse produced by the turn of the inverted sinusoid with the amplitude $S_k U_a$, in the region of $i_a < 0$. In Fig.4, the pulse causing the correction is hachured. Thus, for the constant component, eq.(26) is replaced by

$$I_{a0} = SU\gamma_0(\theta) - SU_1\gamma_0(\theta_1) + S_k U_a \gamma_0(\theta_1). \qquad (32)$$

Let us now discuss the corrections to be made in the formulas for the components of the first harmonic of the plate current. This correction is correlated with the symmetric hatched pulse in Fig.4. Because of the symmetry of this pulse, it contains no quadrature component, so that the correction must be made only in eq.(29) for the active component, whereas eq.(30) for the reactive component holds for the pulse in Fig.4. Thus, for the active component of the first harmonic of the plate current pulse presented in Fig.4, eq.(29) is replaced by

$$I_{a1a} = S(U_c\cos\varphi - DU_a)[\gamma_1(\theta) - \gamma_1(\theta_1)] - S_k U_a[\gamma_1(\theta_1) - \gamma_1(\theta_2)]. \qquad (33)$$

We must also introduce an analogous correction into the first formula for the active component of the upper harmonics:

$$I_{ana} = SU\cos n\psi\gamma_n(\theta) - SU_1\cos n\psi_1\gamma_n(\theta_1) + S_k U_a\gamma_n(\theta_2). \qquad (34)$$

The second formula (31) for the reactive component of the upper harmonics remains unchanged.

The final step is the determination of harmonic components for the pulse presented in Fig.5. In this case, the technique of resolving a complex pulse into elementary semipulses will be applied, using the above resolution ratio of elementary semipulses.

The pulse in Fig.5 can be presented as the sum of the following semipulses: a flat semipulse with cutoffs θ and θ' located at the right of the axis of the control-voltage sinusoid, and a rectangular semipulse of the same height with a cutoff ψ located to the left of the control-voltage axis. From these pulses we must deduct the inverted flat semipulse with cutoffs θ_1' and θ_2 lying close to the right of the sinusoid of the plate voltage U_a. On this basis, the following formula can be developed for the constant component of the plate current pulse presented in Fig.5:

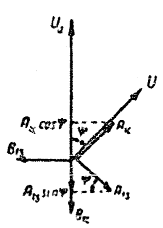

Fig.9

$$I_{a0} = \frac{1}{2} SU\,[\gamma_0(\theta) - \gamma_0(\theta') + \alpha_0(\varphi)(\cos\theta' - \cos\theta)] -$$

$$- \frac{1}{2} S_g U_a\,[\gamma_0(\theta_1') - \gamma_0(\theta_2)]. \qquad (35)$$

Here and in Fig.5, for the sake of brevity, we use the denotations

$$\theta' = \theta_1 + \varphi_1 - \varphi,$$
$$\theta_1' = \theta_1 + \varphi_1.$$

Let us now determine the components of the first harmonic of the plate current. We will denote the cophasal and quadrature components of the first harmonic intrinsic to the first two above semipulses by A_{1c} and A_{1s}, respectively. From the pulse in Fig.5, we obtain the following expressions for A_{1c} and A_{1s}:

$$\left.\begin{aligned} A_{1c} &= \frac{1}{2} SU\,[\gamma_1(\theta) - \gamma_1(\theta') + \alpha_1(\varphi)(\cos\theta' - \cos\theta)] \\ A_{1s} &= SU\,[\gamma_{1s}(\theta) - \gamma_{1s}(\theta') + \alpha_{1s}(\varphi)(\cos\theta' - \cos\theta)] \end{aligned}\right\}. \qquad (36)$$

Having denoted by B_{1c} and B_{1s} the cophasal and quadrature components of the inverted semipulse relative to the voltage on the load (U_a), we obtain the following expressions for these components:

$$\left.\begin{aligned} B_{1c} &= \frac{1}{2} S_g U_a\,[\gamma_1(\theta_1') - \gamma_1(\theta_2)] \\ B_{1s} &= S_g U_a\,[\gamma_{1s}(\theta_1') - \gamma_{1s}(\theta_2)] \end{aligned}\right\}. \qquad (37)$$

In Fig.9 we present a vector diagram to illustrate the phase correlations which must be taken into consideration in constructing formulas for the first harmonic components of the plate current. Figure 9 indicates that both components A_{1c} and A_{1s} give active and reactive current components relative to the voltage U_a. Thus we get the following expressions for the first-harmonic components of the plate current:

$$\left.\begin{aligned} I_{a1a} &= A_{1c}\cos\psi - A_{1s}\sin\psi - B_{1c} \\ I_{a1p} &= A_{1c}\sin\psi + A_{1s}\cos\psi - B_{1s} \end{aligned}\right\} \qquad (38)$$

If we substitute eqs.(36) and (37) into eq.(38) and take into account the two first identities (28), we obtain the following formulas for the first-harmonic components of the plate current:

$$\begin{aligned} I_{a1a} = {} & \frac{1}{2} S(U_c\cos\psi - DU_a)[\gamma_1(\theta_1) - \gamma_1(\theta') + \alpha_1(\psi)(\cos\theta' - \cos\theta_1)] - \\ & - SU_c\sin\psi[\gamma_{1s}(\theta_1) - \gamma_{1s}(\theta') - \alpha_{1s}(\psi)(\cos\theta' - \cos\theta_1)] - \\ & - \frac{1}{2} S_k U_a[\gamma_1(\theta'_1) - \gamma_1(\theta_1)]; \end{aligned} \qquad (39)$$

$$\begin{aligned} I_{a1p} = {} & \frac{1}{2} SU_c\sin\psi[\gamma_1(\theta_1) - \gamma_1(\theta') + \alpha_1(\psi)(\cos\theta' - \cos\theta_1)] + \\ & + S(U_c\cos\psi - DU_a)[\gamma_{1s}(\theta_1) - \gamma_{1s}(\theta') - \alpha_{1s}(\psi)(\cos\theta' - \cos\theta_1)] - \\ & - \frac{1}{2} S_k U_a[\gamma_{1s}(\theta'_1) - \gamma_{1s}(\theta_1)]. \end{aligned} \qquad (40)$$

In a similar manner, we can construct formulas for the upper-harmonic components of the plate current. Thus, instead of eq.(38), we obtain for the upper harmonics:

$$\left.\begin{aligned} I_{ana} &= A_{nc}\cos n\psi - A_{ns}\sin n\psi - B_{nc} \\ I_{anp} &= A_{nc}\sin n\psi + A_{ns}\cos n\psi - B_{ns} \end{aligned}\right\} \qquad (41)$$

Since the structure of these formulas is clear, there is no need to describe them in greater detail.

It should be noted that in calculating pulses like the one presented in Fig.5, we often get $\psi > \theta'_1$, i.e., $\theta' < 0$. In this case, eqs.(35)-(41) hold; we must only take into account that the resolution ratios for the constant components, and also for the cophasal components, are odd functions of the cutoff angle, whereas the

STAT

resolution ratios for the quadrature components are even functions of the cutoff angle, i.e.,

$$\gamma_n(-\theta) = -\gamma_n(\theta),$$

where n = 0,1,2,...;

$$\gamma_{ns}(-\theta) = \gamma_{ns}(\theta),$$

where n = 1,2... .

BIBLIOGRAPHY

1. Dwork, L.E. - Maximum Tank Voltage in Class C Amplifiers. Proc. IRE, No.6, (1950)
2. Khvilivitsky, T.G. - Calculations for a Vacuum-Tube Oscillator Operating in Overvoltage Conditions on a Detuned Load, Radiotekhnika, No.4 (1953)
3. Khmelnitsky, E.P. - A Method for Increasing the Oscillatory Power and Efficiency of Oscillators Operating in Overvoltage Conditions Radiotekhnika, No.8 (1955)
4. Margolin, M.G. - Analysis of the Vacuum-Tube Oscillator as a Current Oscillator Thesis (1946)
5. Model, Z.I., Ivanov, B.I., Person, S.V. and Solovyov, G.F. - Raising the Efficiency of a Powerful HF Vacuum-Tube Oscillator by Separation of the Third Harmonic Radiotekhnika, No.4 (1947)
6. Drobov, S.A. - Radio Transmitters Voyenizdat (1951)
7. Evtyanov, S.I. - Radio Transmitters (1950)

Article received by the Editors on 2 November, 1955.

THEORY OF THE IDEAL RECEIVER

BY

A.A.KHARKEVICH

The noise resistance of receivers whose action is described by two different definitions is investigated.

It is shown that a given receiver may yield better results, depending on the distribution of probabilities of noise.

Section 1. In examining the problem of noise resistance from the geometric point of view, we note that together with an increase in $n = 2FT$ (F being the width of the signal spectrum and T the period of the latter), the noise vector is localized in such a way that, at any given probability, the received signal arranges itself in a spherical stratum (in n-dimensional space) limited by the radii $\rho \pm \varepsilon$, where ρ is the radius of the interference (noise) expressed by the following correlation:

$$\rho = \sigma\sqrt{n} = \sqrt{nP_n} = \sqrt{E_n};$$

where σ is the root-mean-square value of the noise, and P_n and E_n the power and energy of the noise.

In the limit where $n \to \infty$, all the received signals, with a probability that differs infinitely little from unity, lie on the surface of an n-dimensional sphere having a radius of ρ (more accurately, in an infinitely thin spherical stratum).

This circumstance, which has been repeatedly noted in the literature, brings us to the natural idea of using a receiver which detects the actually transmitted signal in the place where it is to be found with the greatest probability, i.e., at the smallest distance from ρ. The action of this kind of receiver is essentially different from the ideal receiver in terms of V.A.Kotelnikov. For this latter we have:

Definition I. The receiver (ideal receiver in terms of Kotelnikov) identifies

STAT

Declassified in Part - Sanitized Copy Approved for Release 2012/10/31 : CIA-RDP81-01043R001300170001-4

the received signal with that of the possible transmitted signals to which it is closest.

On the other hand, for the above-described receiver, we can formulate the following:

Definition II. The receiver identifies the received signal with that of the possible transmitted signals to which the distance closest approaches ρ.

The receivers corresponding to these definitions will be denoted as receivers I and receiver II. Our task will consist in comparing the noise resistance of these two receivers. We will express the noise resistance through the probability of error.

Section 2. Let us first write the general formulas for the error probabilities we will be using.

From the geometric point of view the error probability is the probability that the point of the received signal falls within the region of the n-dimensional signal space in which the receiver identifies the received signal not with the actually transmitted signal but with some other possible signal. We will denote this region by V and call it the region of errors.

It must be pointed out that the difference in the definitions of the receivers reduces to a difference in the boundaries of the region V, as will be explained below.

The probability of error is calculated by means of integrating the n-dimensional density of distribution of the noise probabilities corresponding to the region V.

In Cartesian coordinates, we have

$$P_{err} = \int_V \varphi(x_1, x_2, \ldots x_n) dV, \qquad (1)$$

where $dV = dx_1, dx_2 \ldots dx_n$.

In some cases it is convenient to use polar coordinates. For example, in normal distribution and with uncorrelated noise values, we have

$$\varphi(x_1, x_2, \ldots, x_n) = \frac{1}{(\sqrt{2\pi}\,\sigma)^n} \exp\left(-\frac{1}{2\sigma^2}\sum_{k=1}^{n} x_k^2\right) = \frac{1}{(\sqrt{2\pi}\,\sigma)^n} \exp\left(-\frac{r^2}{2\sigma^2}\right),$$

where $r = \sqrt{\sum_{k=1}^{n} x_k^2}$ is the distance from the point of the transmitted signal. Taking r as one of the variables, we can select the volume element in the form:

$$dV = \theta_n r^{n-1} dr,$$

where $\theta_n = \theta_n(\vartheta)$ is the angular dimension of the n-dimensional segment with an aperture angle of ϑ. Thus, for a noise with normal distribution (fluctuation noise, gauss noise):

$$p_{error} = \frac{1}{(\sqrt{2\pi}\,\sigma)^n} \int_V r^{n-1} e^{-\frac{r^2}{2\sigma^2}} \theta_n dr. \tag{2}$$

Introducing a new variable

$$x = \frac{r}{\sqrt{2}\,\sigma} = \sqrt{\frac{n}{2}}\,\frac{r}{\rho},$$

we get

$$p_{error} = \frac{1}{\pi^{n/2}} \int_V x^{n-1} e^{-x^2} \theta_n dx. \tag{3}$$

The function $x^{n-1}e^{-x^2}$ expresses the distribution along the radius; this function has a maximum at $x = \sqrt{\frac{n}{2}}$, i.e., for $r = \rho$. As for the function $\theta_n(\vartheta)$, it expresses the distribution along the angle and can be defined as

$$\theta_n(\vartheta) = \omega_{n-1} \int_0^{\vartheta} \sin^{n-2} u\, du. \tag{4}$$

where ω is the angular dimension of the sphere of the corresponding number of dimensions, i.e.,

$$\omega_n = \frac{\pi^{\frac{n}{2}}}{\Gamma\left(\frac{n}{2}+1\right)} \qquad (5)$$

These formulas are sufficient for our needs.

Section 3. Let us find the error probability under conditions of gauss noise for the two types of receivers in the simple case where there are only two possible signals a and b represented by two points in n-dimensional space at a distance d from each other. Let us suppose that the signal a is transmitted. For the receiver I, the error probability is determined by the probability with which the point of the received signal is closer to b than to a. Thus, the region of errors for the receiver I represents the half-space limited by a plane equidistant from a and b. In Fig.1, the region of errors is hachured.

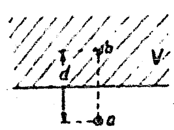

Fig.1

Using eq.(1) and integrating along one coordinate (directed along ab) from $\frac{d}{2}$ to infinity, and along the rest in infinite limits, we obtain the error probability for the receiver I as follows:

$$p_1 = \frac{1}{2}\left[1 - \Phi\left(\sqrt{\frac{n}{2}}\,\lambda\right)\right]. \qquad (6)$$

*λ is introduced on the supposition that the distance d between the signals changes proportionally with a change in ρ. If, on the other hand, d is constant, then eq.(6) can be replaced by

$$p_1 = \frac{1}{2}\left[1 - \Phi\left(\frac{d}{2\sqrt{2}\sigma}\right)\right]$$

i.e., where d is constant, the error probability is not dependent on n.

where

$$\lambda = \frac{d}{2\rho}, \quad \Phi(x) = \frac{2}{\sqrt{\pi}} \int_0^x e^{-z^2} dz.^*$$

Let us now turn to the receiver II. By definition, an error will occur if (Fig.2)

$$|r_1 - \rho| > |r_2 - \rho|. \qquad (7)$$

We get the equation for the error region boundary by replacing the inequality sign in eq.(7) with an equality sign. This gives

$$(r_1 - \rho)^2 = (r_2 - \rho)^2.$$

Utilizing the correlation

$$r_2^2 = r_1^2 + d^2 - 2 r_1 d \cos \vartheta,$$

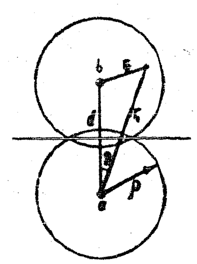

Fig.2

we obtain a quadratic equation for r_1 whose solution is

$$r_{11} = \frac{d}{2} \cdot \frac{1}{\cos \vartheta}. \qquad (8)$$

$$r_{12} = \rho \cdot \frac{1 - \lambda^2}{1 - \lambda \cos \vartheta}. \qquad (9)$$

The first of these two solutions gives an equation of the boundary plane equidistant from a and b. The second solution is the equation of an ellipsoid. Juxtaposing eq.(8) and (9), we obtain the structure for the region of errors as shown in Fig.3. The region of errors is hachured (signal a is transmitted); this region is subdivided into two parts, one of which, V_1, lies inside the ellipsoid (9), while

STAT

the second, V_2, lies outside it. A quick glance at Figs.1 and 3 suffices to show that computing the error probability for the receiver II is considerably more complicated than for the receiver I.

In Fig.4 we show the volume element:

$$dV = \theta_n(\vartheta) r^{n-1} dr,$$

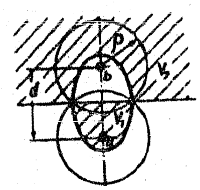

Fig.3

where θ_n is determined by eq.(4), and the value of ϑ is determined by the boundary equation, i.e., for example, for Fig.4 from eq.(9). Moreover, over the area of region V_1, the analytical expression of the boundary angle ϑ changes twice, namely;

for $\quad 0 < r < \rho - \frac{d}{2} \qquad \vartheta = \pi;$

for $\quad \rho - \frac{d}{2} < r < \frac{d}{2} \qquad \vartheta = \arccos \frac{1}{\lambda}\left[1 - \frac{\rho}{r}(1 - \lambda^2)\right];$

For $r > \frac{d}{2}$ the segment loses its top and the angular dimension must be expressed by the corresponding difference. The case of region V_2 is analogous.

Under such circumstances it is easier to make the computation by a numerical method, relying on the sketch. We first prepare graphs or Tables of the angular measures $\theta_n(\vartheta)$. The angle ϑ is measured directly in accordance with the sketch (as in Fig.4). After finding the angular measure, we introduce it by way of a numerical multiplier into eq.(5) and compute the integral as a sum, giving small increments to the radius (e.g., 0.1 ρ). In this way we are able to obtain numerical results; some of these, together with those calculated from eq.(6), are presented in Fig.5. The graph shows the error probability as a function of the parameter $\lambda = \frac{d}{2\rho}$ for different values of n. The solid lines refer to the receiver I and the broken lines to the receiver

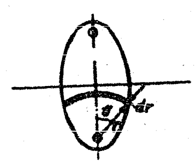

Fig.4

II. It is easily understood that, according to definition, the action of the two receivers does not differ if $\lambda > 1$. As for the interval $0 < \lambda < 1$, the noise re-

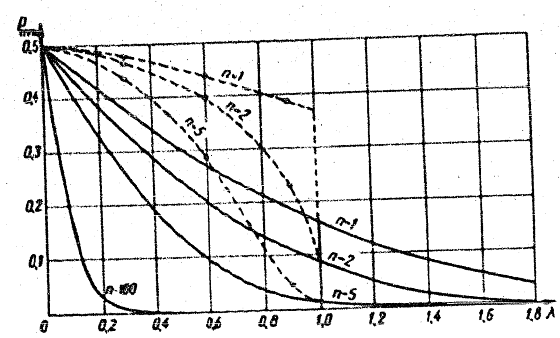

Fig.5

sistance of the receiver II is always lower than that of the receiver I (i.e., $p_{II} > p_I$).

Section 4. We can suppose that this result is specific for the given circuit containing only two possible signals. To verify this supposition let us examine other circuits, e.g., a circuit in which the given signal is surrounded by 2n possible other signals located at the nodes of an n-dimensional cubic lattice. A two-dimensional model of this arrangement is depicted in Fig.6. For the receiver I, the region of errors is represented by the entire space except the n-dimensional cube with sides equal to d (Fig.7). The error probability is determined by the formula

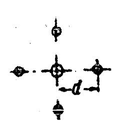

Fig.6

$$p_I = 1 - \Phi^n\left(\sqrt{\frac{n}{2}}\,\lambda\right).$$

For the receiver II, the regions of error for different values of λ are shown in Figs.8, 9, and 10. The results of computing by this method are given in Fig.11.

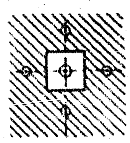

Fig.7

The computations are rather laborious; we therefore, give graph for only m = 1 and 2. Here we can note that the broken lines (receiver II) in some areas dip below the solid lines (receiver I). However, this only occurs for large error probabilities, and is therefore of no practical significance. We also computed the error probability for one value of λ for the arrangement shown in Fig.12. The results are marked in Fig.11 by crosses.

As we see, in all the examined cases, the receiver II is inferior to the receiver I. This result probably is general, although its analytical basis could not yet be defined because of the above-mentioned difficulties.

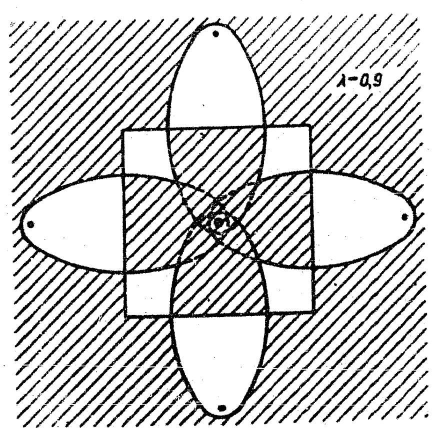

Fig.8

Section 5. We should note, however, that the above conclusion was obtained for a definite type of noise, namely for noise with a normal distribution. The picture changes radically when another distribution is involved. To illustrate this, let us examine a rough but simple example: Let us suppose that the noise is characterized by the fact that its instantaneous power constitutes the mean. This property is exhibited by a double signal, for which only two values are possible: a positive and negative one; they are equal in absolute magnitude. Thus, let us suppose that the useful signal is ± a, and that the noise is also a double signal ± b. Let us look at the two-dimensional case, i.e., a

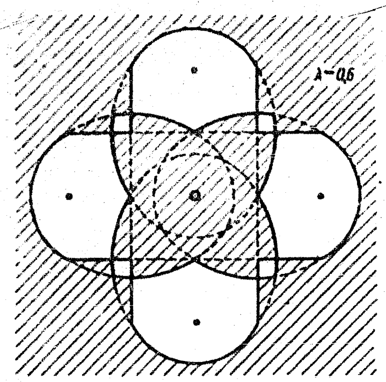

Fig.9

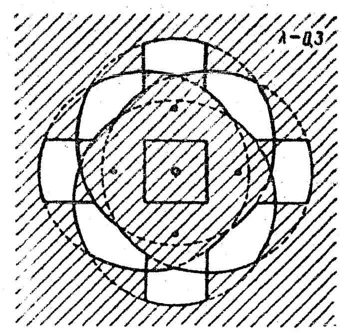

Fig.10

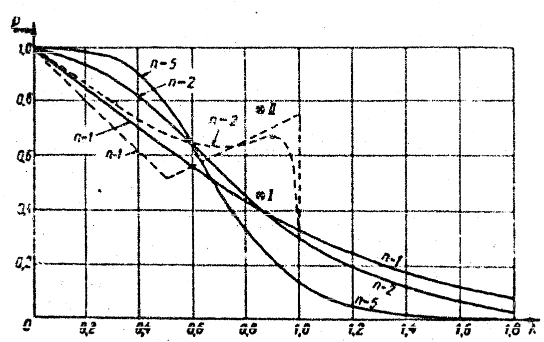

Fig.11

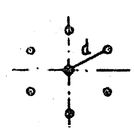

Fig.12

two-valued signal. Four two-valued signals are possible (+a, +a); (+a, -a); (-a, +a); (-a, -a). Let the signal (+a, +a) be transmitted. As a result of the position of the noise, four received signals can be formed: (a+b, a+b); (a+b, a-b); (a-b, a+b); (a-b; a-b). This is shown in Fig.13 for two cases, namely: $b < a$ and $b > a$. The possible transmitted signals are depicted by points and the actually transmitted one by a circle; the possible received signals are shown by crosses.

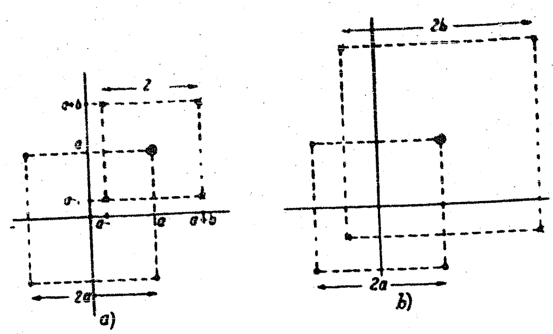

Fig.13

It is easy to see that the condition for correct reception for the receiver I is expressed by the inequality $b < a$. For the receiver II, on the other hand, the condition for correct reception is $b \neq a$. Thus, for the correlations presented in Fig.13b, the receiver I will give an error with a probability of $p_1 = 0.75$. The receiver II, on the other hand, under the conditions of Fig.13b, permits identifying the received signal with the actually transmitted signal. Its action in this process consists in detecting the transmitted signal at a distance $\sqrt{nP_n} = \sqrt{2b}$ from the received signal. The receiver II, acting in a similar fashion, does not even produce an error in the case where the received signal coincides exactly with one of the possible transmitted signals and especially not with the actually transmitted signal. This situation is obtained in the above example where $b = 2a$ [transmitted signal (+a, +a), received signal (a-b, a-b) = (-a, -a)].

The example, although abstract from the point of view of noise reduction, can be of technical significance with regard to separating signals by volume.

In order to obtain a qualitative criterion as to the influence of the noise distribution on the action of the two receivers, let us examine the case of uniform distribution. It is easily seen that in the two-signal circuit, the receivers I and II give identical results. This follows from the fact that the area of the region of errors, as obvious from a comparison of Figs.1 and 3, is identical for both receivers.

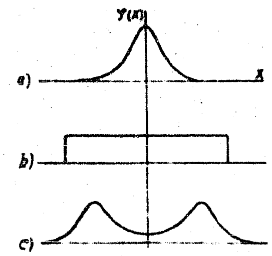

Fig.14

From the above statements we can draw the following conclusion: in a two-signal circuit, in the case of a distribution of the type in Fig.14a, the receiver I is superior to the receiver II; in the case of a distribution as in Fig.14b they are equal; in the case of a distribution as in Fig.14c, the receiver II may be superior to the receiver I in noise resistance.

Article received by the Editors on January 6, 1956.

TECHNIQUE FOR CALCULATING DISPERSION BETWEEN THE FREQUENCIES OF SHORT-WAVE RADIOTELEGRAPH STATIONS

BY

V.M.ROZOV

A technique is described for calculating the protective coefficients necessary to compensate the influence of fadings on the operating stability of short-wave radio communications and the deviation between the carrier frequencies; in this process, the real characteristics of the receiving circuits and the necessary operational quality of the communication are considered.

The protective coefficients proposed by the Provisional Frequency Board are discussed and the inadequacy of the coefficient for the case of doubled reception is demonstrated.

The recommendations of the Provisional Board on determining the frequency deviation between radiotelegraph stations, and also the protective coefficient taking account of fading, were obtained by calculation and, for various special cases, do not correspond to practical requirements.

A comparison of these recommendations with experimentally determined requirements can be made by utilizing the results of an experimental check on the operation of a standard receiver system in the presence of interference from a station operating on an adjacent frequency.

For this purpose, we constructed a model of a radiotelegraph receiver system (Fig.1) satisfying all demands of existing systems.

To the input of the system we applied amplitude- or frequency-keyed voltages simulating the operation of the desired or interfering stations. The input level of

STAT

the desired station signal was selected considerably higher than the level of extrinsic and intrinsic noises of the system; in the absence of a voltage from the jamming station or at a voltage level lower than that of the desired station signal, this arrangement permits the telegraph apparatus of the receiving system to record the transmitted communication without error.

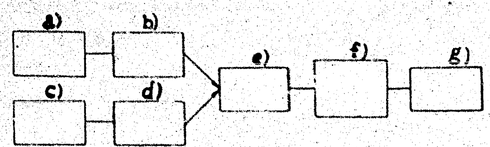

Fig.1

a) Telegraph apparatus; b) GSS-transmitter of desired station; c) Simulator of telegraph signals; d) GSS-transmitter of interfering station; e) Receiver (AR-88 or KTF); f) Tonal amplifier-rectifier (TUV); g) Telegraph apparatus.

On raising the level of the interfering station signal to a given value, no distortion occurs. However, as soon as this level is exceeded by even a small amount, distorted signs begin to appear and then increase sharply.

The ratio of the desired signal level to the interfering signal level, at which distortions appear will be designated the border signal-to-noise ratio and denoted by k_{rp}.

For different deviations of the carrier frequencies of the desired and interfering stations, p_o, under conditions of constant tuning of the receiving system, the magnitude of k_{rp} does not remain constant but is a function of this deviation: $k_{rp} = f(p_o)$.

In Fig.2 we present experimentally obtained graphs showing the function $k_{rp} = f(p_o)$ for receiving systems using KTF-1 receivers under conditions of amplitude and frequency keying of the desired and interfering signals (Curves 2, 3, and 4) and AR-88 with amplitude keying of these signals (Curve 1). The telegraphing speed was 50 bauds.

For convenience, we will assume that the experimental curves in Fig.2 satisfactorily approximate the straight lines 1' and 2' (in a logarithmic system of coordinates).

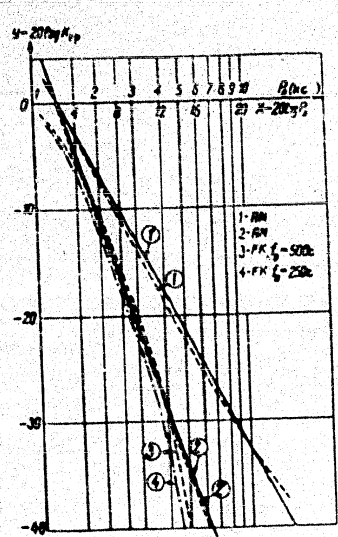

Fig.2

The equations for these curves are

$$\left.\begin{array}{ll} 1)\ y = -1.85\,(x - 2.3) & (\text{AR-88}) \\ 2)\ y = -2.92\,(x - 2.3) & (\text{KT}\Phi\text{-1}) \end{array}\right\} \quad (1)$$

where $x = 20 \log p_0$ and $y = 20 \log k_{rp}$.

Determining x from these equations and then expanding into a power series, we obtain the necessary mathematical formulas for determining the minimum frequency deviations of the desired and interfering stations, as a function of k_{rp};

$$\left.\begin{array}{l} p_0 = 1.3\, k_{rp}^{-0.540};\ k_{rp} < 1 (\text{AR-88}) \\ p_0 = 1.3\, k_{rp}^{-0.342};\ k_{rp} < 1 (\text{KT}\Phi\text{-1}) \end{array}\right\} \quad (2)$$

In finding the minimum deviation with these formulas it is necessary, instead of k_{rp}, to substitute the magnitude of the given signal-to-noise ratio:

$$\left.\begin{array}{ll} p_0 = 1.3\, \alpha^{-0.540} & (\text{AR-88}) \\ p_0 = 1.3\, \alpha^{-0.342} & (\text{KT}\Phi\text{-1}) \end{array}\right\} \quad (2a)$$

where α is the ratio of the mean values of the field levels of the desired and interfering stations.

To calculate the necessary deviation p_0 in the case of signal fading from the desired and interfering stations on condition of a given operational quality of the radio link (estimated from the average percentage of distorted signals), we utilized the results of a statistical analysis of the influence of frequency-adjacent telegraph stations on the operation of a telegraph system (Bibl.1).

In carrying out this analysis we found that interfering stations, as far as frequency is concerned, are located on both sides of the desired station with equal deviation between them; the mean values of the fields (voltages at the receiver input) from the frequency-nearest interfering stations are equal. Here, as was shown previously (Bibl.1), we take into account only the influence of the two interfering stations that are closest in frequency to the desired station, this being sufficient to give a final error of no more than 5-10%. The maximum transmission rate of all stations are assumed to be identical.

In estimating the operation quality of the radio connection in accordance with the probability of the inequality $k < k_{rp}$, where k is the instantaneous value of the signal-to-noise ratio at the input of the receiving system, or in accordance with the average percent of distorted signals over a long period of time, we can come to the conclusion that these two estimates coincide numerically if, in the analysis, the function $\overline{\Pi} = f(k)$ is approximated by the jump function:

$$\Pi(k) = \begin{cases} 1 & \text{for } k < k_{rp} \\ 0 & \text{for } k > k_{rp} \end{cases}$$

The average percentage of distorted symbols in the presence of the above conditions and at single reception is expressed by the following formula:

$$\overline{\Pi} = \frac{2}{3} k_{rp}^2 a^2; \quad k_{rp}^2 a^2 \leqslant 1. \qquad (3)$$

In double reception and under the same conditions, the average percentage of distorted symbols can be calculated by the formula:

$$\overline{\Pi} = \frac{1}{6} k_{rp}^2 a^2; \quad k_{rp}^2 a^2 \leqslant 1. \qquad (4)$$

To obtain a formula for the minimum deviation of the carrier frequencies p_0 in the presence of fadings it is sufficient to eliminate the magnitude of k_{rp} from eq.(3) or (4) and substitute it into eq.(2).

After the necessary computations, we get

for single reception

$$\left.\begin{aligned} p_0 &= 1{,}3\cdot\alpha^{0{,}540}\cdot\left(\frac{3}{2\Pi}\right)^{0{,}270} \quad (\text{AR-88}) \\ p_0 &= 1{,}3\,\alpha^{0{,}342}\cdot\left(\frac{3}{2\Pi}\right)^{0{,}171} \quad (\text{КФТ-1}) \end{aligned}\right\} \qquad (5)$$

for double reception

$$\left.\begin{aligned} p_0 &= 1{,}3\,\alpha^{0{,}540}\left(\frac{3}{2\Pi}\right)^{0{,}270}\cdot 0{,}687 \quad (\text{AR-88}) \\ p_0 &= 1{,}3\,\alpha^{0{,}342}\left(\frac{3}{2\Pi}\right)^{0{,}171}\cdot 0{,}790 \quad (\text{КТФ-1}) \end{aligned}\right\} \qquad (6)$$

The results of calculations of the minimum required deviation are presented in conjunction with eqs.(5) and (6) for the magnitudes of $\Pi = 10^{-3}$, 10^{-4}, 10^{-5} and $\alpha = 10^{-2}$, 10^{-1}, 1.10 and 100 in Table 1; the magnitudes of the minimum deviation are indicated in kilocycles.

Table 1

	α \ Π	AR-88 10^{-3}	AR-88 10^{-4}	AR-88 10^{-5}	КТФ-1 10^{-3}	КТФ-1 10^{-4}	КТФ-1 10^{-5}
a)	10^2	—	—	—	22,0	31,6	48,3
	10	32,5	61,0	—	10,0	14,4	22,0
	1	9,37	17,5	32,5	4,55	6,53	10,1
	10^{-1}	2,70	5,02	9,35	2,07	2,98	4,55
	10^{-2}	—	1,71	3,19	—	1,35	2,07
b)	10^{+2}	—	—	—	17,4	25,0	38,2
	10	22,3	42,0	—	7,90	11,4	17,4
	1	6,43	12,0	22,3	3,60	5,17	8,0
	10^{-1}	1,85	3,45	6,42	1,64	2,36	3,60
	10^{-2}	—	1,18	2,20	—	1,07	1,64

a) Single reception; b) Double reception

From the Table, for the given ratios of average field levels of the desired and interfering stations and the operating quality of the communications lines, we can select the minimum necessary dispersion.

From the expressions (2a), (5), and (6) we can determine the protective coeffi-

147

cient, showing how many times we must increase the signal-to-noise ratio on a radio line with fading over that on a radio line without fading, at a given operating quality of the line. For this, we must find the ratio of the α magnitudes from eq.(5) and from eq.(6) to the α magnitudes from eq.(2a) under conditions of identical deviation p_o.

The results of this calculation are compiled in Table 2.

Table 2

$\overline{\Pi}$	a)	
	b)	c)
10^{-3}	32	26
10^{-4}	41	35
10^{-5}	52	46

a) Protective coefficient (in db); b) in single reception; c) in double reception

The recommendations of the Provisional Frequency Board specify for the protective coefficient at amplitude keying and operating speeds of 120 bauds:

in single reception 40 db

in double reception 25 db.

Conclusions

The method described above for calculating the frequency deviation in radiotelegraph stations and the protective coefficients for compensating the influence of fading takes into account the operating characteristics of the receiving systems and the necessary operating quality of the radio line. As a result, can give conclusions that are more applicable in practical operation.

The protective coefficients recommended by the Provisional Frequency Board correspond to an operating quality of $\overline{\Pi} = 10^{-4}$ in single reception and of $\overline{\Pi} = 10^{-3}$ in double reception.

To meet the present specifications for the operating quality of radio communi-

[redacted] STAT

cations of $\Pi = 10^{-4}$, a protective coefficient in double reception of 35 db must be adopted.

BIBLIOGRAPHY

1. Rozov, V.M. - Thesis, MEIS, 1955.

Article received by the Editors on 3 January 1956.

CONTROL OF RADIO BROADCASTING TRANSMISSION BY MEAN-SQUARE VALUE INDICATORS AND PEAK VALUE INDICATORS*

BY

B.S.MINTZ

The absence until now of a standard indicator for visual volume control in radio broadcasting resulted in unsatisfactory volume adjustment. As a result, radio broadcasting stations and wire broadcasting centers either work below their full power or operate with distortions.

The paper printed below discusses the results of a project carried out in West Germany, comparing volume indicators with various time characteristics. The paper presents factual material which will doubtless be of interest to technicians of radio broadcasting stations and wire broadcasting centers.

The Editor

Introduction

In German radio broadcasting, the standard volume indicator used is a peak meter (pulse meter) of the U21 type with an integration time of about 10 msec, or, as it is also called, a modulation depth meter (Aussteuerungsmesser 48). In the USA since 1938 the standard volume indicator is the familiar mean-square value instrument, type VU, with an integration time of 200 msec.

For a correct estimate of the difference in the indications of these instruments (caused by the difference in their dynamic properties and observed in practical use), we recorded their indications with self-recorders whose dynamic properties

---

* Excerpt from a paper by Pavel (Bibl.1).

were analogous to the dynamic properties of the volume indicators.

In order to verify to what extent the indications of peak values are distorted in the case of the peak meter of modulation depth with an integration time of 10 msec, we also used a modulation depth meter with a rapid self-recorder (integration time approximately 1 msec).

Diagrams and Electric Properties of Instruments

1. Peak Indicator (Pulse Meter U21)

The basic diagram is shown in Fig.1.

Basic properties of instrument:

Integration time at 90% fidelity	10 msec
Return time of pointer from 100% to 10% (switched)	1 or 2 sec
Deviation of pointer	10%
Frequency range	30-15,000 cps
Output resistance	30 k-ohms
Input voltage for pointer deflection to 100%	1.55 eff v or 3.1 eff v
Measuring range	55 db

The modulation depth is usually recorded by a portable measuring instrument which has a wide-range scale and is constructed either in the form of a device with an optical scale with a scale length of about 170 mm (Fig.2) or in the form of an ordinary pointer device of 100 mm diameter (Fig.3). The measuring device itself also contains a pointer system, which is generally used only for calibrating.

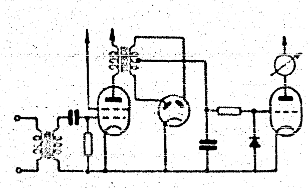

Fig.1

The instrument is calibrated either by means of a built-in circuit or by means of an externally applied sinusoidal voltage. The calibration points are the 1% and 100% marks. The scale of the pulse meter U21 is approximately logarithmic so that the upper and lower amplitude boundaries can be observed with almost identical accuracy. The reading is facilitated by the rapid pick-up and the relatively long return time. The indications in the U21

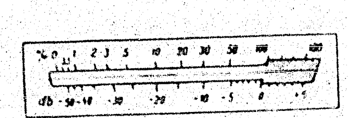

Fig.2

Fig.3

instrument are in direct relation to the stationary sinusoidal voltages used in establishing the level or measuring the level of the transmission system in the normal manner. It is possible to combine several measuring instruments and self-recorders, and also to render the instrument sufficiently sensitive for measuring the noise voltages.

2. Mean-Square Value Indicator Type VU

The basic diagram of the VU (Volume Indicator) instrument is shown in Fig.4. The instrument consists of a tubeless measuring circuit and a rectifier with a gal-

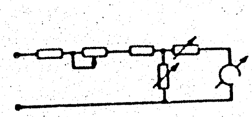

Fig.4

Fig.5

vanometer, and also a ladder attenuator graduated over 2VU (2 db). Recording of the modulation depth is also obtained in accordance with this attenuator. The recording of indications according to the galvanometer scale should only take place next to the mark 0 VU.

STAT

Declassified in Part - Sanitized Copy Approved for Release 2012/10/31 : CIA-RDP81-01043R001300170001-4

The attenuator is set in such a way that the full-scale deflection of the pointer during the observation time (whose duration depends on the type of program) coincides accurately with the point of relative zero level, i.e., the mark M = 100% (accordingly, 0 VU in Fig.5). The instrument is thus calibrated subjectively.

The most important properties of the instrument are as follows: If the instrument input is suddenly supplied with a sinusoidal voltage, of a frequency from 35 to 10,000 cps and an amplitude giving an indication of 0 VU = 100% under stationary conditions, the pointer should, within 300 msec ± 10%, show 99% of the stationary indication at a deviation of not less than 1% and not more than 1.5%. The return time of the needle should not differ greatly from the pick-up time. The input resistance is 7500 ohms or 600 ohms. The instrument has two-half-period rectification with a characteristic index of 1.2 ± 0.2. The scale is approximately linear. The measuring range extends from +4VU to +26VU and is established by means of the above-mentioned attenuator.

The integration time of the VU instrument is more than 20 times as high as the integration time of the U21 pulse meter and reaches a value which, according to experimental data, does not guarantee direct and correct measurement of short but disturbing amplitude peaks of the transmitted program. Such instruments actually measure the mean value, which depends mainly on the dynamic properties of the measuring instrument and is in no mathematical relation with the voltage exciting the system.

"The average durations of pulses" in different programs differ greatly so that the instrument reading depends to a relatively great extent on the nature of the program.

To demonstrate the fact that the VU instrument readings correspond to dynamic measurements under certain conditions dictated by the instrument, the inventors introduced a new measuring unit, the "Volume Unit" (VU), which corresponds numerically to 1 db. The relative zero level point is the volume of a normal program, measured by the VU instrument, where the pointer deflects to the mark 0 VU, rather than the

575

sinusoidal voltage.

In practice it was found that the VU instrument, at maximum amplitudes of a normal program, only gives a deflection 8 — 14 db lower than the pointer deflection for a stationary sinusoidal reference tone with the same maximum amplitude. The range of the instrument indications is thus 6 db.

Taking into account the dispersion from 8 to 14 db, it is necessary in practice, that the pointer deflection of the VU instrument, in measuring by a tone, be at least 10 db greater than the deflection at the maximum peaks of the program.

Comparison of Pick-Up and Integration Curves

The indications of instruments for modulation depth measuring depend essentially on the pick-up curves of the indicator devices and the integration curves of these systems.

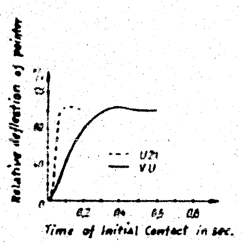

Fig.6

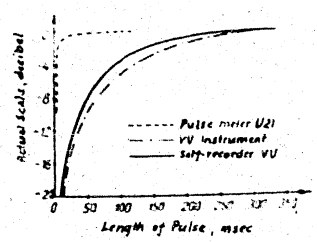

Fig.7

The curves for the pick-up of the galvanometers (Fig.6) show that the galvanometer of the pulse meter U21 has the shortest lag (in round figures, 70 msec as against 300 msec for the VU instrument). These curves illustrate the relation between the pointer deflection of the galvanometer and the action period of the corresponding devices. Because of the short pick-up time of U21 pulse meter at simultaneous acoustic control of the program, the visual sign does not lag noticeably.

In Fig.7 we show curves for the integration of the VU instrument and U21 pulse

STAT

meter. It is obvious that the U21 pulse meter measures pulses having a duration of $t_i \geqslant 10$ msec with considerable accuracy with an error of about 1 db, whereas the VU instrument, at a pulse of 10 msec duration shows about 20 db less.

From an examination of the integration curve of the VU instrument and from a study of the distribution of its readings we can draw the conclusion that the average duration of the pulse of a normal program is about 50 msec, whereas the duration of the shortest pulses equals about 5 msec.

From the integration curve of the VU instrument it follows that its indications should be highly dependent on the type of program.

Experimental Setup

In Fig.8 we show the diagram of the instruments used in the experiment. The program source was a radio broadcasting line or a magnetophone; to adjust the volume we used an attenuator. In addition, the block diagram shows a pulse meter with an indicator having an optical scale; a recording optical instrument AM(10) whose integration time is 10 msec; a pulse meter with rapid self-recorder AM(1) (recording on wax) whose integration time is 1 msec; and an instrument with a self-recorder. From the curves in Fig.7 the degree of approximation of the dynamic performance of the indicator and self-recorder can be estimated. The indications of the self-recorder were slightly more accurate than those of the VU instrument.

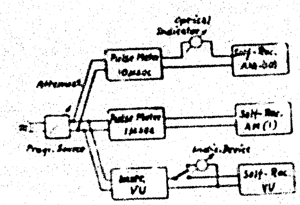

Fig.8

By means of a rapid self-recorder determined whether the pulses of a duration of $t_i < 10$ msec exert a perceptible influence on the growth of indications when measuring peak values on a normal radio program. By means of the three self-recorders the same program was recorded simultaneously.

The speed with which the paper strip moved in each self-recorder was adopted generally as 0.2 mm/sec. To increase the resolving power in the particularly important parts, the speed could be increased to 1 or 5 mm/sec. To facilitate a comparison of the recordings, the common attenuator was adjusted in such a way that the maximum amplitudes reached the 100% mark of the U21 pulse meter [AM(10)].

Experimental Results

During the experiment the three self-recorders recorded widely differing programs. These recordings showed that, for those programs with relatively long pulse periods, the VU instrument gives indications that are too high, whereas the indications of the pulse meters with integration times of 10 msec and 1 msec coincide.

In recording music from Wagner's "Rienzi Overture", the VU instrument raised the indications from about 3 to 6 db. During music played on the xylophone, the VU instrument showed on the average 3 db more than the U21 pulse meter. In recording the sound of footsteps on gravel, the VU instrument in one instance showed 2 db more and in another instance 7 db less than the indications of the pulse meter. At the same time, the indications of the self-recorder (10) were lower by 1-3 db than those of the AM(1). This signifies that the given program also contained impulses shorter than 10 msec.

In measuring the sound effect of horse-galloping produced by two coconut shells, the VU instrument lowered the indications by 7 db, whereas the difference in indications between AM(10) and AM(1) was about 1 db. This means that the pulse duration is 10 msec $\leq t_i < 50$ msec. In recording the ringing of small bells, all three self-recorders showed approximately the same results. The pulse duration in this case corresponds approximately to the adopted value of 50 msec.

In recording speech, the indications of the VU instrument coincided approximately with the indications of the pulse meter, whereas in recording the music which followed directly after the speech, the VU instrument raised the indications to about 3 db.

In recording a spoken broadcast in Hungarian with two speakers, the VU instrument showed approximately identical values for one of the speakers; for the second speaker, the VU instrument lowered the indications from 4 to 6 db. In recording speech in Czech the reverse case occurred: The VU instrument made a considerable positive error, raising the indications to 5 db.

These measurements permit the following conclusions:

a) At a previously assigned 10 db rise in sensitivity in the VU instrument, for a normal program with "pulses of average duration", the positive errors are approximately equal to the negative errors. Consequently, this rise in sensitivity corresponds approximately to practical requirements.

b) The distribution of indications in the VU instrument with regard to peaks measured by the AM(10) instrument is about ± 7-9 db.

c) In rare cases the indications of the AM(10) instrument with integration time 10 msec still do not correspond to the actual voltage peaks.

In spoken broadcasts, the error in the indications of the VU instrument can have both positive and negative signs. It is, therefore, impossible to imagine that some given correction in sensitivity could bring about the difference in the indications of the VU instrument relative to the peak instrument during the broadcasting of a mixed program (speech and music, different speakers on one program).

Conclusions

In radio broadcasting, the peak value gives a more exact picture of the modulation depth of the broadcasting system than the volume determined by the indications of the VU instrument.

Due to the fact that the indications of the VU instrument have no direct relation to the current, voltage or power, a new unit was introduced, the "Volume Unit" (VU). This unit, however, lacks the important property of independence of the measuring device, this being the basic defect of the VU instrument, especially in the trend to replace subjective measuring methods by objective types.

The VU instrument is suitable in cases where no high requirements are made as to accurate control of the modulation depth or where there is a large amplitude reserve and no need to fear distortions from overmodulation. In addition, the instrument can be used on very long radio broadcasting lines for establishing the volume during broadcasting if this line cannot be freed for measurements by sinusoidal current.

In controlling radio broadcasts in terms of the peak instrument, the average operating loudness of the loudspeakers in the receiving sets is dependent on the nature of the program. When the volume is maintained by the VU device, the listener does not need to keep track of the average loudness of his radio set. However, when working with the VU-type instrument there is no assurance of the absence of overmodulation. Therefore, wishing to preserve high quality, the operator often establishes a low modulation level in the transmitter and thus lowers its average distance of action in amplitude modulation. If the given distance of action must be preserved, the possibility of overmodulation exists, which lowers the broadcasting quality.

Without going into details, it should be recalled that FM radio receivers are very sensitive to overmodulation, and when the maximum frequency deviation is exceeded unpleasant distortions develop. The use of VU devices in this case is even more unfavorable than in AM radio broadcasting.

The modern vacuum-tube indicator of peak values can have a logarithmic scale with a large range of indications, which gives it a certain advantage in controlling modulation depth in the studio. It also permits detecting of extraneous voltages in radio broadcasting channels.

In using the peak device, the modulation depth of a transmitting system can be fully utilized, without having to fear a lowering of the quality of the broadcast due to overmodulation. Use of this type of device makes it possible to decrease the "amplitude reserve" in technical equipment and thus to realize considerable economy.

341

BIBLIOGRAPHY

1. Pavel, E.A., Gastell, A., and Bidlingmaier, M. - Comparative Measurements with a Volume Meter and a Peak Meter in Control of Radio Broadcasts. Fernmelde-technische Zeitschrift, No.4 (1955).

Article received by the Editors on 18 January 1956.

NEW METHOD FOR CALCULATING LOSSES IN CYLINDRICAL CONDUCTORS DUE TO THE PROXIMITY EFFECT

BY

V.N.KULESHOV

A new, simplified method of developing formulas for calculating losses in cylindrical conductors is presented, and an example for calculating the resistance of a circuit is given, taking the proximity effect into consideration.

Introduction

The first theoretical study of the propagation of electromagnetic waves through two parallel conductors taking account of the proximity effect, was made by the German Scientist **Mie** (Bibl.1). However, the series he obtained as a result of his study are virtually unusable for practical computations.

Thirty years later, the American scientist Carson (Bibl.2) improved these series somewhat, but did not bring them to the point where they were suitable for practical calculations. Later the English physicist Betterworths (Bibl.3) offered a formula that was completely suitable for practical calculation of the resistance of a pair of conductors. A comparison of the calculation results obtained with the Betterworths and Carson formulas showed that, to calculate the supplementary resistance of a pair of conductors in the frequency range up to 50 kc with adequate accuracy, the Betterworths formula (Bibl.4) can be used. At higher frequency, however, as experiments showed, this formula gives slightly deflated results.

If we take into consideration that at present the packing range of cable communications circuits goes as high as 550 kc and can be even further enlarged, the need for a method for engineering calculation of the resistance of a circuit in the range of higher frequencies is obvious. Below we present a new, simplified method for calculating the resistance of a pair of conductors, this method being suitable in the frequency range up to 1 megacycle.

Differential Equations of the Electromagnetic Field and Solution Methods

The electromagnetic field formed around the conductor influencing the circuit in a communications cable is described by the Maxwell differential equation:

$$\operatorname{rot} E = -\frac{dB}{dt} \text{ and } \operatorname{rot} H = \delta, \qquad (1.1)$$

where E is the intensity of the electrical field,

H is the intensity of the magnetic field,

B is the induction of the magnetic field,

δ is the current density

Equation (1.1) for sinusoidal current in a cylindrical system of coordinates (r, φ, z) is expressed as follows:

$$\left.\begin{aligned} \frac{1}{r}\frac{\partial E_z}{\partial \varphi} - \frac{\partial E_\varphi}{\partial z} &= -i\omega\mu H_r, \\ \frac{\partial E_r}{\partial z} - \frac{\partial E_z}{\partial r} &= -i\omega\mu H_\varphi, \\ \frac{\partial E_\varphi}{\partial r} + \frac{E_\varphi}{r} - \frac{1}{r}\frac{\partial E_r}{\partial \varphi} &= -i\omega\mu H_z \end{aligned}\right\}. \qquad (1.2)$$

$$\left.\begin{aligned} \frac{1}{r}\frac{\partial H_z}{\partial \varphi} - \frac{\partial H_\varphi}{\partial z} &= (\sigma + i\omega\varepsilon)E_r, \\ \frac{\partial H_r}{\partial z} - \frac{\partial H_z}{\partial r} &= (\sigma + i\omega\varepsilon)E_\varphi, \\ \frac{\partial H_\varphi}{\partial r} + \frac{H_\varphi}{r} - \frac{1}{r}\frac{\partial H_r}{\partial \varphi} &= (\sigma + i\omega\varepsilon)E_z \end{aligned}\right\}. \qquad (1.3)$$

where σ is the specific conductivity,

ε is the dielectric permeability,

μ is the magnetic permeability

Equation systems (1.2) and (1.3) can be solved by various methods, but the simplest is the method of separating longitudinal components.

From the field equations (1.2) and (1.3), with the aid of two other Maxwell equations

$$\operatorname{div} E = 0 \qquad (1.4)$$

$$\operatorname{div} H = 0 \qquad (1.5)$$

we easily obtain, for the longitudinal field components, differential equations of the second order

$$\Delta E_z = k^2 E_z, \qquad (1.6)$$

$$\Delta H_z = k^2 H_z, \qquad (1.7)$$

where Δ is the differential operator, determined by the equality

$$\Delta = \frac{\partial^2}{\partial r^2} + \frac{1}{r}\frac{\partial}{\partial r} + \frac{1}{r^2}\frac{\partial^2}{\partial \varphi^2} + \frac{\partial^2}{\partial z^2}; \qquad (1.8)$$

while k is the parameter characterizing the electromagnetic properties of the medium

$$k^2 = i\omega\mu(\sigma + i\omega\varepsilon). \qquad (1.9)$$

In order to solve the wave equations (1.6) and (1.7) we assume that the field changes along the axis z by the rule $e^{-\gamma z}$; which is the case in the great majority of cases of cable technology. Then the radial and circular components of the intensities of the electromagnetic field can be expressed through particular derivatives of the longitudinal components E_z and H_z:

$$E_r = \frac{1}{q^2}\left(\gamma \frac{\partial E_z}{\partial r} + i\omega\mu \frac{\partial H_z}{r\partial \varphi}\right), \qquad (1.10)$$

$$E_\varphi = \frac{1}{q^2}\left(\gamma \frac{\partial E_z}{r\partial \varphi} + i\omega\mu \frac{\partial H_z}{\partial r}\right); \qquad (1.11)$$

$$H_r = \frac{1}{q^2}\left[-(\sigma + i\omega\varepsilon)\frac{\partial E_z}{r\partial \varphi} + \gamma \frac{\partial H_z}{\partial r}\right], \qquad (1.12)$$

$$H_\varphi = \frac{1}{q^2}\left[(\sigma + i\omega\varepsilon)\frac{\partial E_z}{\partial r} + \gamma \frac{\partial H_z}{r\partial \varphi}\right], \qquad (1.13)$$

where γ is the propagation constant characterizing the degree of change of the electromagnetic field along the axis z, and $q = \sqrt{k^2 - \gamma^2}$.

The general solutions to eqs.(1.6) and (1.7) can be presented in the following form (Bibl.5):

$$E_z = \sum_{n=0}^{\infty} [A_n I_n(qr) + B_n K_n(qr)](C_n \cos n\varphi + D_n \sin n\varphi)\, e^{-\gamma z}, \qquad (1.14)$$

$$H_z = \sum_{n=0}^{\infty} [A'_n I_n(qr) + B'_n K_n(qr)](C'_n \cos n\varphi + D'_n \sin n\varphi)\, e^{-\gamma z}, \qquad (1.15)$$

where A_n, $B_n \ldots C'_n$ and D'_n are integration constants,

$I_n(qr)$ and $K_n(qr)$ are modified Bessel function of the first and second kind.

Boundary Conditions

The solutions for the differential equations (1.2), (1.3), (1.5), and (1.6) should satisfy the boundary conditions of the investigated problem.

A communications cable represents a system of conductors isolated from one another by some dielectric and contained in a common lead jacket or armor. Consequently, inside the cable there are several regions filled with different media having nonidentical electric and magnetic parameters (σ, ε, μ).

To determine the field intensity at any given point of the space occupied by the cable, we must find the solution for each region of this space. The solutions, in this case, usually differ from each other by the parameters of the medium and the integration constants and only in some cases by the kind of functions resulting from the general solutions.

To find the integration constants we use the following concepts:

1. In the center of the conductor, when the coordinate $r = 0$, the field intensities have finite values. In this case, the particular solutions expressed through the functions $K_n(qr)$ should be absent.

2. At points lying at infinity, the field intensities vanish. On the basis of this and for an unlimited region, the particular solution expressed through the function $I_n(qr)$ should be absent.

3. On the boundary of two regions, the tangential components of the field intensities are continuous. On the basis of this we can write the following equalities:

$$E_{z1} = E_{z2}, \quad H_{\varphi 1} = H_{\varphi 2} \tag{2.1}$$

$$H_{z1} = H_{z2}, \quad E_{\varphi 1} = E_{\varphi 2} \tag{2.2}$$

in which we presuppose that the axis z is directed along the axis of the conductor

STAT

and that the conductor has a cylindrical shape.

4. On the boundary of two regions, the normal components of the streams of vectors are uninterrupted. On the basis of this, we can write the following correlations:

$$(\sigma_1 + i\omega\varepsilon_1)E_{r1} = (\sigma_2 + i\omega\varepsilon_2)E_{r2}, \tag{2.3}$$

$$i\omega\mu_1 H_{r1} = i\omega\mu_2 H_{r2}. \tag{2.4}$$

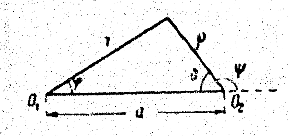

Fig.1

In order to satisfy the boundary conditions, we must often make a conversion of the field from one cylindrical system of coordinates to another with the center on the axis of the investigated conductor. To convert the coordinates, it is useful to make use of the following formulas:

$$r = \sqrt{(a + \rho e^{i\psi})(a + \rho e^{-i\psi})} = \sqrt{(a - \rho e^{i\vartheta})(a - \rho e^{-i\vartheta})}, \tag{2.5}$$

$$\rho = \sqrt{(a - re^{i\varphi})(a - re^{-i\varphi})}, \tag{2.6}$$

where a is the distance between the centers of the coordinates,

ψ is the external angle,

ϑ is the internal angle (Fig.1).

Method of Superimposing Reflected Waves

The method of superimposing the reflected waves is widely used in studying the propagation of electromagnetic energy along air lines. This permits studying the complex process of the propagation of electromagnetic energy in a simple and graphic form. The general wave of the voltage or current is resolved into a series of incident and a series of reflected waves. Each of these waves can be studied separately, and since they are presented in a simple form, the general study is considerably facilitated.

In a cable we deal with a uniform medium so that the propagation process of

314

electromagnetic energy inside it is considerably more complex than over an air line. The presence of insulating interlayers and adjacent conductors causes a reflection in radial direction; the presence of nonuniformities along the cable causes reflection in the direction of the cable axis.

Inasmuch as the method of superimposing reflected waves simplifies the examination of complex processes, we will use it to study the electromagnetic field in communications cables.

As an example let us examine a symmetric pair of copper conductors (Fig.2).

Fig.2

Let a current I flow in the conductor a and no current in the conductor b. To simplify the mathematical computation we will also assume that the field is symmetric with respect to the axis of the conductor a and that $\gamma \approx 0$. Then the solution to eqs.(1.14) and (1.15) will look as follows:

$$E_z = AI_0(kr) + BK_0(kr),$$
$$H_z = 0.$$

Let us suppose that the space surrounding the conductor is unlimited; then, A = 0. The integration constant B is determined on the basis of the law of complete current where $r = r_a$. From the equation

$$H_\varphi = \frac{1}{i\omega\mu} \cdot \frac{dE_z}{dr} = -\frac{k}{i\omega\mu} BK_1(kr) = \frac{I}{2\pi r} \qquad (3.1)$$

it follows that

$$B = -\frac{i\omega\mu I}{2\pi r_a k K_1(kr_a)},$$

where r_a is the radius of the conductor a.

Since, in practice, $kr_a \ll 1$, we can consider that

$$E_z = -\frac{i\omega\mu I}{\pi} \ln \frac{kr}{1.12}, \quad (kr < 1). \qquad (3.2)$$

where $1.12 \approx \frac{2}{1.781}$.

The presence of an adjacent conductor distorts the field causing it to become asymmetric. This will lead to a reflected field which we will denote by E'_z. The resultant field will equal the sum, i.e.,

$$E_z = E_{za} + E'_{za}. \qquad (3.3)$$

The subscript a in eq.(3.3) signifies that the field intensities are correlated with the current in conductor a.

The reflected field is asymmetric and is determined by eq.(1.14) in the coordinate system ρ and ϑ.

$$E'_{za} = \sum_{n=0}^{\infty} C_n K_n(k\rho)\cos n\vartheta, \quad (\rho > r_b). \qquad (3.4)$$

where C_n is an integration constant.

There are no particular solutions with sines under conditions of horizontal arrangement of the conductors (Bibl.6).

When $k\rho << 1$, eq.(3.4) is simplified as follows:

$$E'_{za} = C_0 + C'_0 \ln\rho + \sum_{n=1}^{\infty} C'_n \rho^{-n}\cos n\vartheta, \quad (\rho > r_b). \qquad (3.5)$$

where C'_0, C'_n are integration constants differing from C_n in constant multipliers.

Adapting eq.(3.2) to the coordinate system ρ and ϑ in terms of eq.(2.5), we get

$$E_{za} = -\frac{i\omega\mu I}{2\pi}\left[\ln\frac{ka}{1.12} - \sum_{n=1}^{\infty}\frac{1}{n}\left(\frac{\rho}{a}\right)^n \cos n\vartheta\right], \quad a > \rho > r_b. \qquad (3.6)$$

where a is the distance between conductors.

The intensity of the electrical field inside the conductor b is determined in the coordinate system ρ and these, in turn, from eq.(1.14):

$$E_z = \sum_{n=0}^{\infty} D_n I_n(k_b\rho)\cos n\vartheta, \quad (\rho > r_b). \qquad (3.7)$$

where $k_b = \sqrt{i\omega\mu_b\sigma_b}$. The solutions expressed through the function $K_n(k_b\rho)$ are absent in view of the fact that this function, where $\rho = 0$, does not satisfy the condition of finite value.

Substituting eqs.(3.5) and (3.6) into eq.(3.3) and equating, on the basis of eq.(2.1), the outside field to the field inside conductor b where $\rho = r_b$, we will

STAT

have:

$$C_0 + C_0' \ln r_b + \sum_{n=1}^{\infty} C_n' r_b^{-n} (\cos n\theta - \frac{i\omega\mu I}{2\pi} \left[\ln \frac{ka}{1.12} - \sum_{n=1}^{\infty} \frac{1}{n} \left(\frac{r_b}{a}\right)^n \cos n\theta \right] =$$

$$= \sum_{n=0}^{\infty} D_n I_n (k_b r_b) \cos n\theta. \qquad (3.8)$$

For the intensities H_ϑ we will also have

$$\frac{C_0'}{i\omega\mu r_b} - \frac{1}{i\omega\mu} \sum_{n=1}^{\infty} n C_n' r_b^{-n-1} \cos n\theta + \frac{I}{2\pi} \sum_{n=1}^{\infty} \left(\frac{r_b}{a}\right)^{n-1} \cos n\theta =$$

$$= \frac{k_b}{i\omega\mu_b} \sum_{n=0}^{\infty} D_n I_n' (k_b r_b) \cos n\theta. \qquad (3.9)$$

Since, in the conductor b the over-all current equals zero, we have

$$\int_0^{2\pi} H_\vartheta r_b d\theta = 0.$$

Consequently,

$$C_0' = D_0 = 0.$$

In order for the boundary conditions to be satisfied at any point on the surface of the conductor b, we must equate the coefficients in eqs. (3.8) and (3.9) to sines

$$C_0 - \frac{i\omega\mu I}{2\pi} \ln \frac{ka}{1.12} = 0,$$

$$C_n' r_b^{-n} + \frac{i\omega\mu I}{2\pi} \frac{1}{n} \left(\frac{r_b}{a}\right)^n = D_n I_n (k_b r_b),$$

$$-\frac{n}{i\omega\mu} C_n' r_b^{-n-1} + \frac{I}{2\pi} \left(\frac{r_b}{a}\right)^{n-1} = \frac{k_b}{i\omega\mu_b} D_n I_n' (k_b r_b),$$

whence it follows that (if $\mu = \mu_b$)

$$\left.\begin{aligned} C_0 &= \frac{i\omega\mu I}{2\pi} \ln \frac{ka}{1.12}, \\ C_n' &= -\frac{i\omega\mu I}{2\pi n} \cdot \frac{r_b^{2n}}{a^n} Z_n, \\ D_n &= \frac{i\omega\mu I}{2\pi n} \left(\frac{r_b}{a}\right)^n \frac{1 - Z_n}{I_n (k_b r_b)}, \end{aligned}\right\} \qquad (3.10)$$

where

$$Z_n = \frac{I_{n+1} (k_b r_b)}{I_{n-1} (k_b r_b)}. \qquad (3.11)$$

First substituting eq.(3.10) into eq.(3.5) and then the result, together with (3.6), into eq.(3.3), will give the value of the electric field intensity if $a \geq \rho \geq r_b$:

$$E_z = \frac{i\omega\mu I}{2\pi}\sum_{n=1}^{\infty}\frac{1}{n}\left[\left(\frac{\rho}{a}\right)^n - \left(\frac{r_b^2}{a\rho}\right)^n Z_n\right]\cos n\theta \qquad (3.12)$$

and the value of the magnetic field intensity

$$H_\theta = \frac{I}{2\pi\rho}\sum_{n=1}^{\infty}\left[\left(\frac{\rho}{a}\right)^n + \left(\frac{r_b^2}{a\rho}\right)^n Z_n\right]\cos n\theta. \qquad (3.13)$$

The coefficient of reflection at the point $\rho = r_b$ takes the value:

$$P_{rb} = \frac{E'_{za}}{E_{za}} = \frac{\ln\frac{ka}{1.12} - \sum_{n=1}^{\infty}\frac{1}{n}\left(\frac{r_b}{a}\right)^n Z_n \cos n\theta}{\ln\frac{ka}{1.12} - \sum_{n=1}^{\infty}\frac{1}{n}\left(\frac{r_b}{a}\right)^n \cos n\theta}.$$

In an analogous manner, we can obtain the values of the fields if $\rho > a$.

Knowing the intensity of the field close to the conductor b, we can determine the apparent power absorbed by this conductor and the supplementary resistance due to losses owing to the proximity effect:

(power per unit length)

$$P_b = \int_0^{2\pi} E_z(k_b r_b) H_\theta^*(k_b r_b)\, r_b\, d\theta = \frac{i\omega\mu I I^*}{4\pi}\sum_{n=1}^{\infty}\frac{1}{n}\left(\frac{r_b}{a}\right)^{2n}(1 - Z_n)(1 + Z_n^*). \qquad (3.14)$$

where the asterisks indicate complexly conjugated magnitudes:

(supplementary resistance per unit length)

$$Z_b = \frac{P_b}{II^*} = \frac{i\omega\mu}{4\pi}\sum_{n=1}^{\infty}\frac{1}{n}\left(\frac{r_b}{a}\right)^{2n}(1 - Z_n)(1 + Z_n^*). \qquad (3.15)$$

Supplementary Resistance of a Symmetric Pair

If a current of the same magnitude as in the conductor a flows through the conductor b, but in the opposite direction, the field near the conductors can be determined by the superposition method. The magnitude of the supplementary resistance for a pair of identical conductors in this case will equal

STAT

$$z_{62} = 2z_6 = \frac{i\omega\mu}{2\pi}\sum_{n=1}^{\infty}\frac{1}{n}\left(\frac{r_0}{a}\right)^{2n}(1 - Z_n)(1 + Z_n), \qquad (4.1)$$

where r_0 is the radius of the conductor.

Designating that $X_n = Re(X_n) + iIm(X_n)$ and substituting the latter into eq.(4.1), we get

$$z_{62} = \frac{i\omega\mu}{2\pi}\sum_{n=1}^{\infty}\frac{1}{n}\left(\frac{r_0}{a}\right)^{2n}[1 - |Z_n|^2 - i2Im(Z_n)]. \qquad (4.2)$$

The material part of eq.(4.2) will equal

$$R_{62} = \frac{\omega\mu}{\pi}\sum_{n=1}^{\infty}\frac{1}{n}\left(\frac{r_0}{a}\right)^{2n}Im(Z_n), \qquad (4.3)$$

and the imaginary part:

$$i\omega L_{62} = \frac{i\omega\mu}{2\pi}\sum_{n=1}^{\infty}\frac{1}{n}\left(\frac{r_0}{a}\right)^{2n}(1 - |Z_n|^2). \qquad (4.4)$$

Equation (4.3) characterizes the supplementary resistance due to losses from eddy currents in the conductors, i.e., the supplementary resistance due to the proximity effect. Experience shows that the series in eq.(4.3) can be limited to two terms. Then the supplementary resistance per unit length of the line can be determined with adequate accuracy by the formula:

$$R_{62} = \frac{\omega\mu}{\pi}\left(\frac{r_0}{a}\right)^2\left[Im(Z_1) + \frac{1}{2}\left(\frac{r_0}{a}\right)^2 Im(Z_2)\right]. \qquad (4.5)$$

Expressing $Im(X_1)$ and $Im(X_2)$ through the moduli and phases of Bessel functions, and substituting the latter into eq.(4.5), we get:

$$R_{62} = R_0\left[\left(\frac{d_0}{a}\right)^2 G(x) + \left(\frac{d_0}{a}\right)^4 F(x)\right], \qquad (4.6)$$

where R_0 is the resistance of two conductors under conditions of direct current:

$$G(x) = \frac{x}{4}\cdot\frac{M_1(x)}{M_0(x)}\sin(\theta_0 - \theta_1 + 135^\circ), \qquad (4.7)$$

$$F(x) = \frac{x}{2}\cdot\frac{M_0(x)}{M_1(x)}\cos(\theta_0 - \theta_1 + 135^\circ) - 1, \qquad (4.8)$$

$$x = \sqrt{\omega\mu_b\sigma_b}\,r_0; \quad d_0 = 2r_0. \qquad (4.9)$$

The values of the functions F(x) and G(x) can also be determined relative to the magnitude of the parameter x using the Tables given in various books (e.g., Bibl.6).

The general expression taking account of the basic resistance of a pair of conductors under alternating current, and the supplementary resistance due to losses produced by the proximity effect of the conductors, can now be written as follows:

$$R = R_0\left[1 + F(x) + \left(\frac{d_0}{a}\right)^2 G(x) + \left(\frac{d_0}{a}\right)^4 F(x)\right]. \qquad (4.10)$$

In Fig.3 we present a comparison of the results calculated from eq.(4.10) (Curve 1) and from the Betterworth formula (Curve 2). The comparison indicates that, at low frequency up to 250 kc, the values of the resistance for a pair of conductors with a diameter of 1.2 mm completely coincide, whereas at high frequency they diverge slightly.

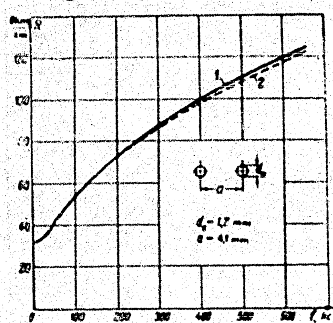

Fig.3

Experience shows that the high results obtained with eq.(4.10) give better agreement with the actual values than the results obtained with the Betterworth formula. This proves the validity of the assumptions made in developing the mathematical formula (4.10). The formula was obtained more easily and requires only two tabular values, F(x) and G(x), instead of the three required for the Betterworth formula.

BIBLIOGRAPHY

1. - Ann. Phys. p.200, 1900.

2. - Phil. Mag. April 1921.

3. - Phil. Trans. Royal Soc. London, v. 222, 1922.

4. - Nauchno-Tech. Sbornik MEIS, No. 1, 1937.

5. - Smirnov,V.I. - Course in Higher Mathematics, vol. 3, Part 2, GITTL (1949)

6. - Kuleshov,V.N. - Theory of Communications Cables, Svyz'izdat (1950)

Article received by the Editors on 8 February 1956.

INCREASE IN MUTUAL INTERFERENCE OF CIRCUITS, DUE TO REFLECTION FROM THE ENDS OF THIRD CIRCUITS

BY

P.K.AKULSHIN

It is demonstrated that, under practical conditions, where all "third" circuits are insulated on both ends, there is an increase in mutual interference of the circuits, both on the far and near ends, due to reflection of current and voltage waves from the ends of the third circuits. Formulas for calculating cross-over circuit arrangements, taking this interference into account, are given. Suggestions are made as to feeding the influence produced by third circuits from the output of one amplifier to the input of the other amplifier.

Introduction

In an article entitled "Mutual Interference of Packed Steel Circuits due to Adjacent T&M Circuits" (Bibl.1) it was pointed out that, if the third circuits are not closed on their wave resistance but left isolated, then on the far end of the second circuit will appear an additional influence produced by the reflection of current and voltage waves from the ends of the third circuits.

Here we must note that all "third" circuits are, in practice, always isolated. In fact, each two-conductor telephone circuit closed on its wave resistance should be regarded as a "single-conductor" circuit, consisting of two parallel conductors, like a "peak" circuit but without connection of the center point with the ground. In view of this, all such "single-conductor" circuits can be replaced by one equivalent single-conductor circuit that is insulated from the ground.

A more detailed study of this matter is given below.

Mutual Interference on Far End due to Reflection of Current and Voltage Waves from Ends of Third Circuits

In Fig.1 we present the first and second two-conductor circuits and a third equivalent single-conductor circuit. Each of these circuits is depicted by one line.

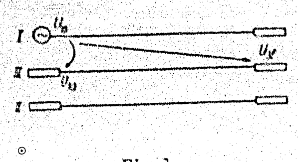

Fig.1

The voltages U_{30} and U_{31} are those obtained on the near and far ends of the third equivalent single-conductor circuit when it is closed on the corresponding wave resistance.

If the ends of this third circuit are insulated, each of the above voltages will be reflected repeatedly from the corresponding ends of the third circuit.

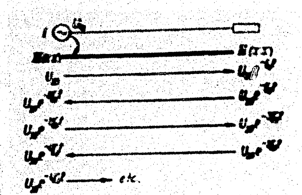

Fig.2

Let us examine separately the repeatedly reflected voltage waves U_{30} and U_{31}.

Under conditions of repeated reflection of the voltage waves U_{30} (Fig.2), the sum of voltage waves running from left to right over the third circuit, i.e., from the near end, will be defined as

$$(U_{30})_0 = U_{30}(1 + e^{-2\gamma_3 l} + \ldots) = \frac{U_{30}}{1 - e^{-2\gamma_3 l}}. \qquad (1)$$

Analogously, for the sum of voltage waves running from right to left, i.e. from the far end, we can write

$$(U_{30})_d = \frac{U_{30}\, e^{-\gamma_3 l}}{1 - e^{-2\gamma_3 l}}. \qquad (2)$$

For U_{30}, we have

$$U_{30} = iU_{10}\frac{\omega Z_3 K_{13}}{2(\gamma_1 + \gamma_3)}(1 - e^{-(\gamma_1 + \gamma_3)l}). \qquad (3)$$

The sum of voltage waves running from left to right will be denoted as the additional influence on the left end (in terms of the law of the near end) and right end (in terms of the law of the far end) of the second circuit. In turn, the sum of voltage waves running from right to left will be denoted as the additional influence on the right end (in terms of the law of the near end) and on the left end (in terms of the law of the far end) of the second circuit. In the given case, we are interested in the influence on the far right end of the second circuit. Neglecting the influence on the right end of the second circuit obeying the law of the far end and using Fig.3 as basis, the voltage on the end of the second circuit U'_{12}, can be expressed as

$$U'_{2l} = i(U_{3l})_d \frac{\omega Z_2 K_{32}}{2(\gamma_3+\gamma_2)}\left(1-e^{-(\gamma_3+\gamma_2)l}\right). \qquad (4)$$

We designate that

$$\left| i\frac{\omega Z_3 K_{13}}{2(\gamma_1+\gamma_3)}\right| = e^{-B_{13}}, \qquad \left| i\frac{\omega Z_2 K_{32}}{2(\gamma_3+\gamma_2)}\right| = e^{-B_{32}},$$

$$B_{132} = B_{13} + B_{32}.$$

Then, substituting the corresponding values into eq.(4) from eqs.(2) and (3) and bearing in mind that $\gamma_1 = \gamma_2$, simple transformations will lead to

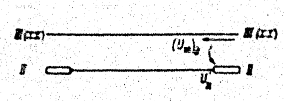

Fig.3

$$U'_{2l} = U_{10} e^{-B_{132}} e^{-\gamma_1 l} \frac{\text{th}\left(\frac{\gamma_1+\gamma_3}{2}\right)l}{1-e^{-2\gamma_1 l}}\left(1-e^{-2(\gamma_1+\gamma_3)l}\right). \qquad (5)$$

It is not difficult to show that, if the first circuit is crossed, eq.(3) will contain an additional multiplier T_I corresponding to the product of tangents, according to the number of subscripts in the cross-over arrangement of the first circuit.

If, in addition, the second circuit is crossed, eq.(4) will contain an analogous multiplier T_{II}.

Consequently, in the general case for crossed first and second circuits we will have

$$U'_{2l} = U_{10} e^{-B_{132}} e^{-\gamma_1 l} \frac{\text{th}\left(\frac{\gamma_1+\gamma_3}{2}\right)l}{1-e^{-2\gamma_1 l}}\left(1-e^{2(\gamma_1+\gamma_3)l}\right) T_I T_{II}. \qquad (6)$$

Since $U_1 = U_{1o}e^{-\gamma_1 l}$, it follows that

$$U_{10} = U_{1l} e^{\gamma_1 l};$$

$$\frac{U_{1l}}{U'_{2l}} = e^{B_{132}} e^{-\gamma_1 l} e^{\gamma_1 l} \frac{1-e^{-2\gamma_1 l}}{\text{th}\left(\frac{\gamma_1+\gamma_3}{2}\right)l} \frac{1}{\left(1-e^{-2(\gamma_1+\gamma_3)l}\right)} \cdot \frac{1}{T_I T_{II}}. \qquad (7)$$

Hence for the shielding of steel circuits we get

$$B'_{sh} = \ln\left|\frac{U_{11}}{U_{21}}\right| = B_{132} - (\beta_1 - \beta_3)\,l + B_l + B_I + B_{II} + A_1 + A_2. \qquad (8)$$

where

$$B_l = \ln\left|\frac{1}{\operatorname{th}\left(\frac{\gamma_1 + \gamma_3}{2}\right) l}\right|; \quad B_I = \ln\left|\frac{1}{T_I}\right|; \quad B_{II} = \ln\left|\frac{1}{T_{II}}\right|;$$

$$A_1 = \ln\left|1 - e^{-2\gamma_3 l}\right|; \quad A_2 = \ln\left|\frac{1}{1 - e^{-2(\gamma_1+\gamma_3)l}}\right|.$$

Under conditions of repeated reflection of the voltage waves U_{31}, analogous to the above, the sum of voltage waves running from right to left is defined as

$$(U_{31})_d = \frac{U_{31}}{1 - e^{-2\gamma_3 l}}, \qquad (9)$$

where

$$U_{31} = iU_{10}\frac{\omega Z_3 K'_{13}}{2(\gamma_3 - \gamma_1)} e^{-\gamma_1 l}\left(1 - e^{-(\gamma_3 - \gamma_1)l}\right). \qquad (10)$$

For the sum of voltage waves running from left to right, we will have

$$(U_{31})_d = \frac{U_{31} e^{-\gamma_3 l}}{1 - e^{-2\gamma_3 l}}. \qquad (11)$$

The sum of voltage waves running from left to right over the third circuit will, analogous to the above, produce an influence mainly on the far end of the second circuit. The latter also is of interest. Bearing this in mind, for a voltage induced on the far end of the second circuit we can write

$$U''_{32} = i\,(U_{31})_d \frac{\omega Z_2 K_{32}}{2(\gamma_3 + \gamma_2)}\left(1 - e^{-(\gamma_3 + \gamma_2)l}\right). \qquad (12)$$

If the first and second circuits are crossed, eqs. (10) and (12) will include the multipliers τ_I and T_{II} respectively, where τ_I is the product of tangents of the type $\tanh\left(\frac{\gamma_3 - \gamma_1}{2}\right) nS$ corresponding to the cross-over indexes of the first circuit, and T_{II} is the product of tangents of the type $\tanh\left(\frac{\gamma_3 + \gamma_2}{2}\right) nS$ corresponding to the cross-over indexes of the second circuit.

We will designate that

$$\left|i\frac{\omega Z_2 K_{32}}{2(\gamma_3 + \gamma_2)}\right| = e^{-B_{32}}; \quad \left|i\frac{\omega Z_3 K'_{13}}{2(\gamma_3 - \gamma_1)}\right|^{*} = A_{13}.$$

* Here, K_{32} and K'_{13} denote the connection factors between circuits for the near and far ends, respectively.

Further, analogous to the above, transformations will yield

$$B''_{sh} = \ln\left|\frac{U_{11}}{U''_{31}}\right| = B_{31} + \ln\left|\frac{1}{A_{13}}\right| - (\beta_1 - \beta_3)l + B'_1 + B_{11} + A_1 + A_3. \tag{13}$$

where

$$B'_1 = \ln\left|\frac{1}{\tau_1}\right|; \quad A_3 = \ln\left|\frac{1}{1 - e^{-(\gamma_1 + \gamma_3)l}}\right|.$$

When the ends of the third circuit are closed on the corresponding wave resistance, the shielding of steel circuit, when crossed in an arrangement without identical maximum indexes, was determined from eq.(14); see (Bibl.2):

$$B_{sh} = \ln\left|\frac{1}{A_{132}}\right| - (\beta_1 - \beta_3)l + B'_1 + B_{11} \tag{14}$$

A comparison of eqs.(8), (13), and (14) shows that all these formulas contain a term $-(\beta_1 - \beta_3)$ which, in the main, decreases the mutual shielding of the steel circuits.

Let us compare the results of calculating the mutual shielding of the remaining circuits with the data of measurements.

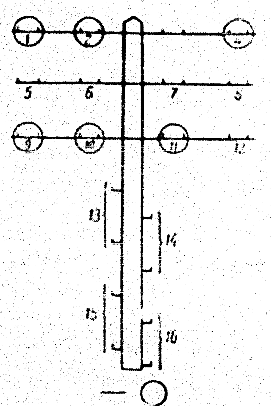

Fig.4

1) TsM circuits; 2) Remaining circuits - steel; 3) Steel circuit No.12 not suspended

The shielding calculations were conducted for one of the interference components, using eq.(8).

The measurements were done by specialists at the TsNIIIS on an experimental line of the Ministry of Communications, on the Golitsyno-Mitkino sector, between the sixth and seventh steel circuits (Fig.4) of which the sixth is not crossed while the seventh is crossed by the index 8 with a length of the elements of 131 m. The length of the experimental line is 128 elements, i.e., 16.8 km. All the third lines - both the steel and the TsM circuits - were insulated on both ends of the lines.

In calculating, the parameters of the third equivalent circuit were adopted as equal to the parameters of a copper two-conductor circuit, d = 4 mm. The magnitude of B_{132} was adopted as equal to 8 nepers.

The gradation of frequencies in the computations was adopted on the basis of the oscillation period of the magnitude of A_1 in eq.(8), i.e., above 4.5 kc. The mathematical curve (Fig.5) was constructed in accordance with this. The measurements were

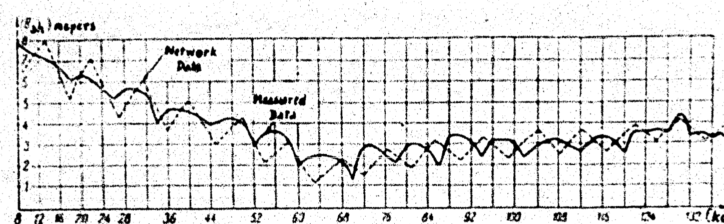

Fig.5

made over 2 kc and from these data we also constructed a curve.

A comparison of these curves shows that both the periodicity of the oscillation of B_{shield} and its absolute values along the curves approach each other rather closely.

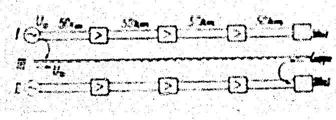

Fig.6

These data also indicate that, under the investigated measuring conditions, the main role is played by the current flowing to the far end of the second circuit, due to voltage reflection U_{30} from the ends of the TsM circuits, since B_{shield}, as determined from eq.(14), decreases evenly over the entire frequency range and has no oscillations. On the other hand, the presence of voltages flowing to the far end over two other paths [cf. eqs.(13) and (14)], at some frequencies change the absolute magnitude of B_{shield}, obviously because of the changing phase of these voltages relative to the phase of voltages from U_{30}.

In practice, when studying the mutual interference of steel circuits and TsM circuits, it must be borne in mind that the TsM circuits, in transit, pass the amplifying point of the steel circuits; therefore, there will be no repeated reflection of voltage waves on the TsM circuits. As shown by Fig.6, at a length of the amplifying section of the TsM circuits of the order of 200 km, the attenuation of these circuits at f = 25 kc will be of the order of 1.5 nepers so that all additional reflected waves, except the fundamental waves, will be attenuated.

Mutual Interference at the Near End due to Reflection of Current and Voltage Waves from the Ends of Third Circuits

The reflection of voltage waves from the ends of third circuits results in an increase in the interference at the near end of the second circuits (Bibl.3).

Figure 7 shows that the reflected voltage wave U_{30}, moving over the third circuit from left to right, will generate an interference voltage U''_{20} on the near end of the second circuit, in addition to the voltage U'_{29} which appears on the near end of the second circuit, due to a direct link between the first and second circuits. This additional voltage will have a greater relative effect, the greater the distance between the first and second circuits becomes. For instance, between the first and second circuits suspended on the first and fourth places of an eight-place cross beam, the quantity B_o = 7.6 nepers, and the magnitude $B_{132} = B_{13} + B_{32}$ equals approximately 8 nepers. In other words, the voltage U''_{20} will have almost the same magnitude as the voltage U'_{20}, in the absence of cross-overs in the first and second circuits. If, on the other hand, the cross-over arrangements of the first and second circuits produce, simultaneously, a large negative effect at some frequencies, the voltage U''_{20} may be many times larger than the voltage U'_{20}; in this case, the transient attenuation on the near end between the first and second circuits will be dependent almost exclusively on the reflection of voltage waves from the ends of the third circuits and may be considerably smaller than the magnitude

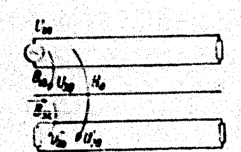

Fig.7

of B_0.

Hence it follows that, in calculating the cross-over arrangements of circuits, so as to avoid increasing the mutual interference of circuits on the near end, due to reflection from the ends of third circuits, the cross-over arrangement of the first and second circuits must not produce a great negative effect.

Let us determine the maximum permissible negative cross-over effect of the first and second circuits for various cases.

We will designate that $B_{12} = \ln\left|\frac{U_{10}}{U'_{20}}\right|$; $B_3 = \ln\left|\frac{U_{10}}{U''_{20}}\right|$.

Then, for electrically long lines, we can write

$$B_{12} = B_0 + B_{I-II}, \qquad (15)$$

$$B_3 = B_{132} + B_I + B_{II}, \qquad (16)$$

where B_{I-II} is the additional magnitude of the transient attenuation in accordance with the indexes of reciprocal cross-overs between the first and second circuits;

B_I and B_{II} are the additional magnitudes of the transient attenuation in accordance with the cross-over indexes of the first and second circuits.

Thus, the transient attenuation between the first and second circuits as a result of the additional influence caused by reflection from the ends of third circuits will be defined as

$$B_{0u} = \ln\left|\frac{U_{10}}{U'_{20} + U''_{20}}\right| = B_{12} - \ln\left[1 + e^{-(B_3 - B_{12})}\right]. \qquad (17)$$

The transient attenuation on the near end (B_{ou}) should satisfy the existing norms; see P. K. Akulshin (Bibl.4), eq.(218).

For a number of amplifying sections equal to 20, B_{ou} = 5.35 nepers.

Further, at a pre-assigned magnitude of B_{12}, the formula for determining B_3 is

$$B_3 = B_{0u} + \ln\frac{1}{1 - e^{-(B_{12} - B_{0u})}}, \qquad (18)$$

whence for $B_{12} = B_{ou} + 0.2$ neper = 5.55 nepers, we have B_3 = 7.06 nepers.and for

$B_{12} = B_{ou} + 0.4$ neper = 5.75 nepers, we have $B_3 = 6.45$ nepers.

These computations show that if between some circuits, we can obtain B_{12} = = 5.75 nepers, the sum of $B_I + B_{II}$ at B_{132} = 8 nepers is determined as

$$B_I + B_{II} = B_3 - B_{132} = (6.45 - 8)\ nep = -1.55\ nepers$$

Otherwise, in this case we can permit a negative cross-over effect of the first and second circuits equal to 1.55 nepers. At B_{12} = 5.55 nepers, this negative effect should not exceed 0.94 neper.

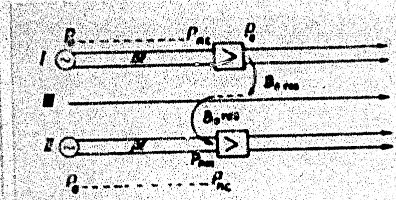

Fig.8

The strictest demands on the cross-over arrangement of each circuit is made by mutual interference of circuits at the amplification points, when the sum of $B_I + B_I$ necessarily will have a positive value.

In fact, Fig.8 shows that, from the output of the first circuit amplifier to the input of the second circuit amplifier a level of transient currents of P_{nm} exists. The mutual shielding of the circuits for this interference path is determined from the correlation

$$B_{sh} = P_{nc} - P_{nm} = (P_0 - \beta l) - (P_0 - 2B_{0\,res}) = 2B_{0\,res} - \beta l. \qquad (19)$$

whence the mean value of the necessary transient attenuation on the near end, between the first and third circuits and between the third and second circuits, equals

$$B_{0\,res} = \frac{1}{2}(B_{sh} + \beta l). \qquad (20)$$

Thus if we adopt the necessary degree of shielding between steel circuits in the amplifying section as equal to 6.5 nepers and the attenuation of the amplifying section of the steel circuit also as equal to 6.5 nepers, the magnitude of $B_{0\,res}$ should be not less than 6.5 nepers. Hence it follows that, in the absence of blocking coils in the conductors of the third circuit, the cross-over arrangement of each circuit of the first and second circuits should give, over the entire range of the

STAT

92

transmitted frequencies, a positive effect of not less than 2.5 nepers. Here we consider that the circuits are suspended on transverse elements and that

$$B_{13} = B_{32} = 4 \text{ nepers}$$

When the circuits are hung on hooks, with the distance between conductors being either 60 or 40 cm, a value of about 3 nepers is obtained for the quantities B_{13} and B_{32}. Then the positive cross-over effect should be not less than 3.5 nepers. Such a positive effect in the range of frequencies transmitted over steel circuits, when they are packed in a three-channel system (up to 25 kc), cannot be obtained in practice; consequently, to satisfy the specifications for shielding, we must either place blocking coils into the conductors of the third circuits or decrease the damping of the amplifying section of the steel circuits, or else change the construction of the line - decrease the distance between the conductors of each circuit and increase the distance between circuits. The latter provision may give an increase in B_{12} and B_{32} of up to 4 nepers.

Between TsM circuits, the question of interference at the amplifying points is even more complex.

Indeed, for 20 amplifying sections we have

$$B_{sh} = 5.8 + \frac{1}{2} \ln N = 7.3 \text{ nepers}$$

At a length of the amplifying section of 100 kc (in a 12-channel system), the attenuation of the amplifying section, in the absence of ice-crusting or hoar frost, where f = 143 kc, can be adopted as 2.4 nepers.

Then, on the basis of eq.(20) we obtain

$$B_{0\,req} = 4.85 \text{ nepers}$$

When the circuits are suspended on transverse elements, $B_{13} = B_{32}$ will equal 4 nepers; consequently, the cross-over arrangement of the first and second circuits should give a positive effect of 0.85 neper each, or

$$B_{I} + B_{II} = 1.7 \text{ nepers}$$

The existing structural inhomogeneities of the lines make it possible to obtain

STAT

102

a positive cross-over effect, where $f \neq 143$ kc, of the order of only 0.4 neper.

Hence it follows that, even in the absence of hoar frost or ice, the shielding of TaM circuits at the amplification points, due to a transition of current through third circuits does not satisfy the norm in the upper part of the frequency range of a 12-channel system by almost a whole neper.

Where there is hoar frost or ice, at which time the attenuation of the amplifying section rises greatly, the mutual shielding of the circuits is decreased even further.

Raising the mutual shielding of circuits can only be done by installing filters and blocking coils in the conductors of third circuits.

In the absence of blocking filters, the sum of $B_I + B_{II}$ over the entire frequency range must have a positive value, at any rate not lower than $2B_{ok}$, thus requiring more frequency cross-overs.

With the aim, on the other hand, of lowering the demands made of the linear devices, it is highly desirable to install noise suppressors at the beginnings and ends of the circuits and to use devices with inversion and frequency shift in the adjacent circuits.

BIBLIOGRAPHY

1. - Electric Communications, No.1 (1956)
2. - Mutual Interference of Packed Steel Circuits due to Adjacent TaM Circuits, Electric Communications, No.1 (1956)
3. Akulshin, P.K., Koshcheyev, I.A., and Kulbatsky, K.E. - Theory of Communications over Conductors. Svyaz'izdat (1940), pp.274-279
4. Akulshin, P.K. - Cross-Over of Telephone Circuits (1953), p.100

Received by the Editors on 6 October 1955.

STAT

DECREASING THE ATTENUATION IN COAXIAL CABLES

BY

K.K.SERGEYEVA

To decrease attenuation in the transmission of HF currents over coaxial cables, we recommend splitting the conductor into separate insulated wires. This structural change in the cable, at certain frequencies, permits a reduction in attenuation of more than twice, relative to the attenuation of a cable with a solid conductor.

Formulas for calculating the basic parameters of the cable are given.

Introduction

In communications lines, an attenuation minimum occurs when the following condition is satisfied:

$$\frac{R}{L}=\frac{G}{C}. \qquad (1)$$

In all actual lines, we have

$$\frac{R}{L}>\frac{G}{C}. \qquad (2)$$

To realize condition (1) in practice, the inductance of the line is artificially increased.

The inductance of a coaxial cable can be increased by galvanically depositing on the inside conductor a thin layer of magnetic material or winding of wire or tape made of material with a high magnetic permeability . However, both these methods are technically complicated. A more practical way of increasing the inductance might be to deposit a layer of magnetic dielectric on the inside conductor.

The theory of such cables has been presented quite fully in works by V.N. Kushelov (Bibl.1), I.A.Koscheyev (Bibl.2), I.E.Efimov (Bibl.3) and other Russian and

205

foreign scientists.

As indicated by Efimov (Bibl.3), a layer of magnetic dielectric will increase the capacitance of the cable and the losses in the magnetic dielectric at high frequencies. As a result of this, the method gives no noticeable decrease in damping.

In the present article, another way of reducing attenuation is described.

In coaxial cables, containing a HF dielectric and operating in a relatively narrow frequency band, the attenuation is basically determined by the energy losses in the conductor material and can be approximately computed by means of the formula

$$\beta = \frac{R}{2}\sqrt{\frac{C}{L}}\ \frac{nep}{km}. \qquad (3)$$

Consequently, to decrease the attenuation we must reduce the resistance R.

In some electric and radio devices, use is made of split conductors. This kind of conductor (Fig.1) consists of a large number of individual, insulated, thin wires wound together in such a way that each of them passes inside and outside the conductor. Such a conductor can be produced by twisting individual wires into groups and then winding several such groups (up to five) together.

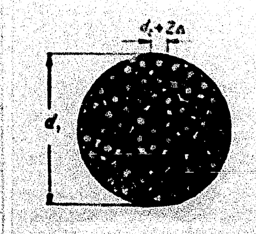

Fig.1

As a result of transposing the wires by sections, each of them is exposed to an identical number of the lines of force of the field. Since the transverse dimensions of the wires are insignificant, the surface effect will manifest itself weakly, i.e., the current density by sections of the wires will be identical everywhere.

The resistance of the split conductor, as shown in Bibl.4, is composed of two quantities and can be determined from the expression:

$$R = R_0(1 + 408 n f^2 \theta d_0^4)\ \frac{ohm}{km}. \qquad (4)$$

In eq.(4), the term R_0 denotes the resistance due to losses produced by the surface effect. We can calculate the magnitude of this resistance, in a given conductor, as the resistance to direct current. The term $408 R_0 n f^2 \theta d_0^4$ is the resistance due to the proximity effect (n is the total number of wires, f the frequency in cps, d_0 the diameter of the wires in terms of the copper in meters), θ is the packing coefficient, i.e., the ratio of the cross-sectional area of the copper to the entire area of the section of the split conductor, while d_1 is the diameter of the conductor in meters.

Let us designate that $A = 406 n f^2 \theta d_0^4$. In the case of a constant diameter of the wires d_0 and constant packing coefficient θ the percentual change in resistance of the split conductor, together with the frequency change, will be proportional to the magnitude of A, i.e., to

$$\frac{R - R_0}{R_0} = A. \tag{5}$$

In selecting the shape of the split conductor it is important that the value of A is as low as possible. When $A \to 0$, $\frac{R}{R_0} \to 1$ and $R = R_0$.

The magnitude of A, at constant frequency, can be reduced considerably by reducing the diameter of the wires d_0 (Fig.2). However, a reduction in d_0 at a constant diameter of the conductor d_1 and constant insulation thickness Δ always results in an increase in the number of wires n. The increase in n can be determined approximately by the formula:

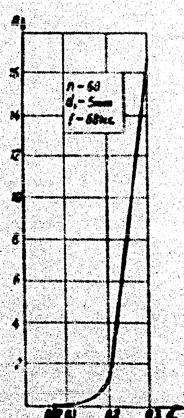

Fig.2

$$m = \frac{3}{4} \frac{d_1^2}{d_0^2 + 4\Delta d_0 + 4\Delta^2} + \frac{3}{2} \frac{d_1}{d_0 + 2\Delta} + 1, \tag{6}$$
$$n = Nm,$$

where m is the number of wires in a group and N is the number of groups.

Since A increases proportionally to n^2, it is impossible, by decreasing d_0, to reduce the magnitude of A significantly. Consequently, on the one hand, the number of wires n should be as small as possible. On the other hand, a reduction in the number of wires n is accompanied by an increase in the term R_0, which is dependent on n in the following manner:

$$R_0 = \frac{R_{0\,spl}}{\eta} = \frac{R_{0\,spl}\, d_1^2}{n d_0^2}\, k, \qquad (7)$$

where $R_{0\,spl}$ is the resistance to direct current of the solid conductor with a diameter of d_1; k is a coefficient characterizing the increase in length of the wires, due to the winding.

Since R_0 and ΔR_0 depend on n differently (Fig.3), we must select an optimum number of wires, which simultaneously assure a minimum value for these terms.

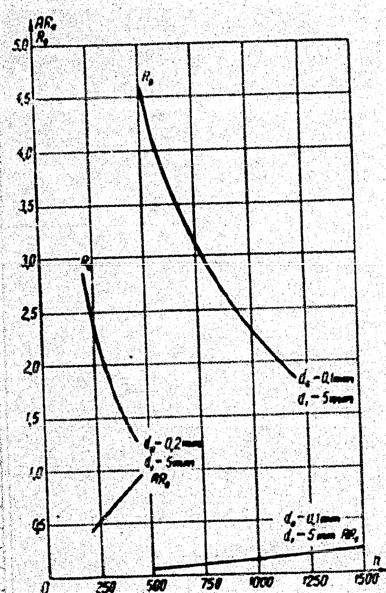

Fig.3

A study of eq.(4) at minimum n shows that the number of wires should equal

$$n_{opt} = \frac{d_1}{20.2 f d_0^3} \qquad (8)$$

From this we see that, for different values of d_0 at constant d_1 and f, the optimum number of wires will vary.

The matter of selecting the optimum number of wires is of interest in the case where the value of the terms R_0 and ΔR_0 in eq.(4) is identical, i.e., where the energy losses caused by the proximity effect are commensurable to or higher than the losses caused by the surface effect.

In the case where the resistance of the split conductor is basically determined by losses due to the surface effect, an investigation of $\frac{dR}{dn} = 0$ is pointless.

Field of Application for Split Conductor

A split conductor does not always have a lower resistance than a solid conductor of the same diameter and operating on the same frequencies. In other words, it is not always possible to replace a solid conductor by a split conductor. If, in the solid conductor, the surface effect is considerable, there is good reason to replace it by a split conductor. We know that the surface effect is greater, the closer the correlation between the penetration depth and the transverse dimension of the conductor. Therefore, an increase in resistance caused by the surface effect in a single conductor occurs, at equal strength, in conductors of small radius but operating at high frequencies, and in conductors of large radius operating at low frequencies.

In other words, there is no reason to replace a solid conductor of 1-2 mm diameter, used at low frequencies, since a split conductor of the same diameter would have greater resistance than a solid conductor. This is to be explained by the fact that, in either conductor, the resistance would be close to the resistance to direct current. The resistance R_o of the split conductor, would be larger than $R_{o\ sol}$ by the magnitude of the packing coefficient, which is always less. However,

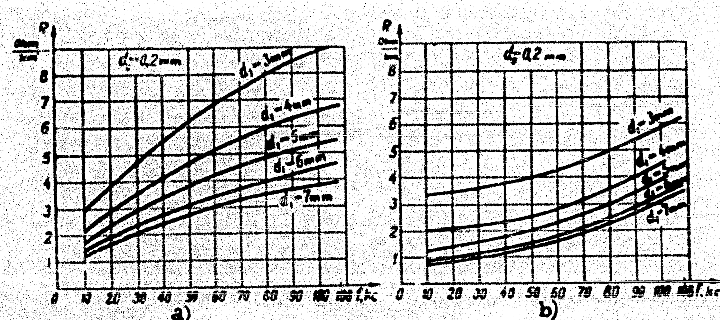

Fig.4

a) Continuous conductor; b) Split conductor

if we now raise the frequency to a given limit, the resistance of the split conductor will increase more slowly than that of the solid conductor. This is illustrated by the curves in Fig.4.

The limitations as to the use of split conductors at very high frequencies can

227

be explained by the sharp rise in losses due to the proximity effect, which losses may by far exceed the losses due to the surface effect.

From the above statements it follows that a split conductor can be used instead of a solid one in the following cases:

1) where the solid conductor has a small diameter but transmits high frequencies;

2) where the diameter of the solid conductor is more than 3 mm and is used at frequencies beginning with 30 kc. The larger the diameter, the smaller will be this starting frequency.

Application of Split Conductors to Coaxial Cables

About 80% of the total resistance of coaxial cables is a component of the resistance of the inside conductor. Because of this, it is advisable to replace the inside conductor. The primary and secondary parameters of cables with split inside conductors can be computed from the following approximate formulas:

Resistance. If the cable is used for a relatively small range, its total resistance is determined by the formula:

$$R \approx \frac{R_{(ap)}\, d_1^2}{n d_0^2} k + 8{,}36 \cdot 10^{-5} \sqrt{f}\, \frac{1}{d_1} \frac{\text{ohm}}{\text{km}} \qquad (9)$$

or by

$$R \approx \frac{4\rho k}{n d_{1\,equiv.}^2} + 8{,}36 \cdot 10^{-5} \sqrt{f}\, \frac{1}{d_1} \frac{\text{ohm}}{\text{km}}. \qquad (10)$$

where d_1 equiv. = $d_0\sqrt{n}$

When the cable operates on higher frequencies, the resistance of the split inside conductor should be determined from eq. (4).

Inductance. We know that the inductance in coaxial cables is composed of the inductances of the inside conductor L_1, of the outside conductor L_2, and of their mutual inductance $L_{1,2}$. Since, together with a rise in frequency, the inductances L_1 and L_2 decrease in ordinary cables, the inductance is basically determined by the magnetic stream between the conductors and equals

$$L = L_{1,2} = 2 \ln \frac{r_2}{r_1} 10^{-4} \frac{\text{henry}}{\text{km}}. \qquad (11)$$

STAT

On the other hand, in a cable with a split inside conductor, the inductance would be larger than in an ordinary cable, due to the increase in the inductance of the inside conductor:

$$L = L_1 + L_{1,2}$$

or

$$L = \left(\frac{1}{2} + 2\ln\frac{r_2}{r_{1\,equiv}}\right) \cdot 10^{-4}\ \frac{henry}{km}, \qquad (12)$$

where $r_{1\ equiv.} = r_o\sqrt{n}$

<u>Capacitance and Conductance of Insulation</u>. In coaxial cables, the capacitance and conductance of the insulation is determined in the same way as in an ordinary cable:

$$C = \frac{\varepsilon_r 10^{-6}}{18\ln\frac{r_2}{r_1}}\ \frac{f}{km}, \qquad (13)$$

$$G = \omega C \operatorname{tg}\delta\ \frac{mohm}{km}. \qquad (14)$$

<u>Wave Resistance</u>. Due to an increase in the inductance, the wave resistance also increases

$$Z = \sqrt{\frac{L}{C}}\ ohm \qquad (15)$$

The attenuation and phase shift are determined by the formulas

$$\beta = \frac{R}{2}\sqrt{\frac{C}{L}}\ \frac{neper}{km}. \qquad (16)$$

$$\alpha = \omega\sqrt{LC}\ \frac{rad}{km}. \qquad (17)$$

<u>Conclusion</u>

The use of split inside conductors in coaxial cables permits a considerable reduction in attenuation. Computations show that, in some types of cables, the attenuation is lowered more than two times. This can be explained by the fact that the use of a split conductor simultaneously lowers the resistance and raises the inductance of the cable. Thus, a transition from the inequality (2) to the condition (1) is realized by a decrease in R and an increase in L.

BIBLIOGRAPHY

1. Kuleshov, V.N. - Theory and Communications Cables, Svyaz'izdat (1950)

2. Koshcheyev, I.A. - Theory and Practical Use of Bimetallic Cores in Communications Cables. Dissertation (1943)

3. Efimov, I.E. - The use of Magnetic Dielectrics for Some Types of Communications Cables. Dissertation (1946)

4. Howe, G.W. - The High-Frequency Resistance of Multiply-Stranded Insulated Wire. Proceedings of the Royal Society of London, Ser. A, Vol.93, No.A 654, (1917)

Article received by the Editors on 20 August 1955.

DISPLACING SIGNAL SPECTRA

BY

A.Y.LEV AND B.I.YAKHINSON

The transformation of a physically realizable signal created on displacement of its spectrum along the frequency scale from one region to another is described, and the reversibility conditions of the transformation are discussed.

The possibility of single-band transmission of signals by displacing their spectrum is reviewed. The basic possibility of synthesizing a signal with a displaced spectrum in accordance with the particular ordinates of the initial signal is demonstrated. In this method, no limitations are placed on its spectrum with regard to the zero and adjacent frequencies.

Solving the basic problems in the technology of electric communications - distance, high reliability, and multichannel operation - is closely correlated with the necessity of transforming the shape of signals. One such transformation is the conversion of the frequency composition of the signal, e.g., in modulation or detection and also in spectrum shifts.

Spectrum Shift

The problem of spectrum shift has been discussed by a number of authors (Bibl.1-4), but this item still needs further discussion.

The problem is formulated as follows: From a pre-assigned signal $f_1(t)$ whose complex spectrum is $S_1(\omega)$ we must determine the real signal $f_2(t)$ corresponding to the spectrum $S_2(\omega)$, which represents the spectrum of the signal $f_1(t)$ shifted along the frequency scale by a magnitude Ω.

The problem is discussed in this form in Bibl.1, where the spectrum shift is represented by the formal operation $S_{\Omega}(\omega) = S_1(\omega - \Omega)$, this being used at all values of ω (Fig.1). By virtue of this, the function $f_{\Omega}(t)$, corresponding to the converted asymmetric spectrum $S_{\Omega}(\omega)$, proves to be complex. This solution, which is irreproachable from the formal point of view, creates the impression that it is impossible to shift the spectrum in real systems; at the same time we know that a spectrum shift from one region to another is frequently done and widely used in communications. Apparently, a spectrum shift should be defined as something different; in any case, the result of the shift should be a spectrum corresponding to the real signal.

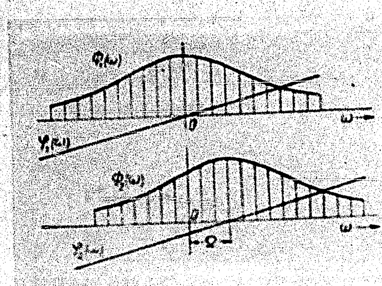

Fig.1

Since any real signal is described by the actual function of an actual variable t, its complex spectrum

$$S(\omega) = \Phi(\omega) e^{i\varphi(\omega)} = \frac{1}{\sqrt{2\pi}} \int_{-\infty}^{\infty} f(t) e^{-i\omega t} dt \qquad (1)$$

is characterized by the fact that $\Phi(\omega)$ and $\varphi(\omega)$ are, respectively, even and odd functions.

Since it is presupposed that, after a spectrum shift, we should obtain the real signal, the spectral characteristic $S_2(\omega)$ should also possess the indicated properties; therefore, in the case of a spectrum shift upward on the frequency scale, we have

$$\left.\begin{array}{ll} S_2(\omega) = S_1(\omega - \Omega), & \omega > \Omega \\ S_2(\omega) = S_1(\omega + \Omega), & \omega < -\Omega \\ S_2(\omega) = 0, & -\Omega < \omega < \Omega \end{array}\right\}. \qquad (2)$$

The corresponding spectral characteristics of the signals which must be and have been converted are shown in Fig.2.

The conversion determining the function f(t) in terms of its spectral characteristic can be written as follows:

$$f(t) = \text{Re}\,\frac{2}{\sqrt{2\pi}}\int_0^\infty S(\omega)e^{i\omega t}\,d\omega. \qquad (3)$$

In accordance with eqs.(2) and (3), the converted signal is to be determined as follows:

$$f_2(t) = \text{Re}\,\frac{2}{\sqrt{2\pi}}\int_0^\infty S_2(\omega)e^{i\omega t}\,d\omega = \text{Re}\,\frac{2}{\sqrt{2\pi}}\int_0^\infty S_1(\omega-\Omega)e^{i\omega t}\,d\omega.$$

Let us introduce the designation $\omega - \Omega = \zeta$; then,

$$f_2(t) = \text{Re}\,\frac{2}{\sqrt{2\pi}}\int_0^\infty S_1(\zeta)e^{i(\zeta+\Omega)t}\,d\zeta,$$

or

$$f_2(t) = \text{Re}\,e^{i\Omega t}\frac{2}{\sqrt{2\pi}}\int_0^\infty S_1(\omega)e^{i\omega t}\,d\omega. \qquad (4)$$

Determining $S_1(\omega)$ from eq.(1), we obtain from eq.(4) a direct relation between the signal that has been converted and that which is to be converted:

$$f_2(t) = \text{Re}\,e^{i\Omega t}\frac{1}{\pi}\int_0^\infty e^{i\omega t}\,d\omega\int_{-\infty}^{\infty} f_1(t)e^{-i\omega t}\,dt. \qquad (5)$$

The investigated operation is reversible. This means that if spectrum $S_2(\omega)$ of the converted signal $f_2(t)$ is reduced the frequency scale by Ω, we will obtain spectrum $S_1(\omega)$ corresponding to the initial signal $f_1(t)$. Thus, regarding the given spectrum shift down the frequency scale as the reverse operation of the upward shift, we can establish the relation between the function to be converted $f_1(t)$ and the converted function $f_2(t)$ in the following way:

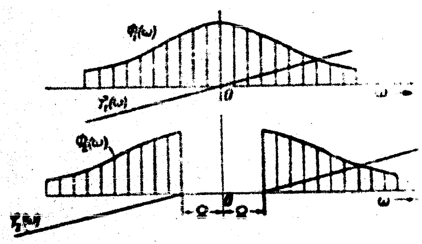

Fig.2

$$f_2(t) = \text{Re}\,e^{-i\Omega t}\frac{1}{\pi}\int_0^\infty e^{i\omega t}\,d\omega\int_{-\infty}^{\infty} f_1(t)e^{-i\omega t}\,dt. \qquad (6)$$

However, spectrum shift down the frequency scale can also be thought of as an independent operation. Here we must examine the problem further. We have in mind the case where Ω, in absolute magnitude, exceeds the lowest frequency in the spectrum of the signal to be converted (Fig.3) and, consequently:

$$\left.\begin{aligned} S_2(\omega) &= S_1(\omega+\Omega), & \omega &> \Omega \\ S_2(\omega) &= S_1(\omega-\Omega), & \omega &< -\Omega \\ S_2(\omega) &= S_1(\omega+\Omega)+S_1(\omega-\Omega), & -\Omega &< \omega < \Omega \end{aligned}\right\} \qquad (7)$$

Let us find the converted signal $f_2(t)$ corresponding to spectrum $S_2(\omega)$ as defined by conditions (7):

$$f_2(t) = \mathrm{Re}\,\frac{2}{\sqrt{2\pi}}\int_0^\infty S_2(\omega)e^{i\omega t}\,d\omega =$$

$$= \mathrm{Re}\,\frac{2}{\sqrt{2\pi}}\left\{\int_0^\Omega [S_1(\omega+\Omega)+S_1(\omega-\Omega)]e^{i\omega t}\,d\omega + \int_\Omega^\infty S_1(\omega+\Omega)e^{i\omega t}\,d\omega\right\}.$$

or

$$f_2(t) = \mathrm{Re}\left[e^{-i\Omega t}\frac{1}{\pi}\int_0^\infty e^{i\omega t}d\omega\int_{-\infty}^\infty f_1(t)e^{-i\omega t}\,dt - iN(t)\right]. \qquad (8)$$

where

$$N(t) = \frac{4}{\sqrt{2\pi}}\int_0^\Omega \Phi_1(\omega)\sin[(\omega-\Omega)t+\varphi_1(\omega)]\,d\omega.$$

Upon finding the converted signal $f_2(t)$, we can omit the term $iN(t)$ in eq.(8), so that, in all cases of spectrum shift, we will have

$$f_2(t) = \mathrm{Re}\,e^{\pm i\Omega t}\frac{1}{\pi}\int_0^\infty e^{i\omega t}\,d\omega\int_{-\infty}^\infty f_1(t)e^{-i\omega t}\,dt. \qquad (9)$$

The plus sign before $i\Omega_t$ in eq.(9) refers to an upward shift and the minus sign to a downward shift on the frequency scale.

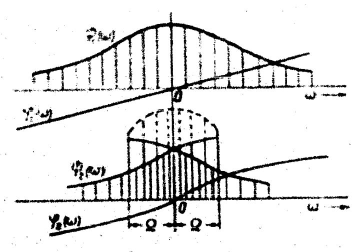

Fig.3

The presence of the term $iN(t)$ in eq.(8), however, points to an irreversibility of the displacement process in the sense defined by conditions (7); in fact, if the spectrum of the converted signal $f_2(t)$ is shifted by Ω down the frequency scale, the signal obtained from this reverse operation will be

$$\mathrm{Re}\,e^{i\Omega t}\left[e^{-i\Omega t}\frac{1}{\pi}\int_0^\infty e^{i\omega t}\,d\omega\int_{-\infty}^\infty f_1(t)e^{-i\omega t}\,dt - iN(t)\right] =$$

$$= f_1(t) + N(t)\sin\Omega t.$$

Thus, a reverse conversion in this case does not lead to the initial signal.

STAT

Single-Band Transmission

The above considerations might be utilized in working on the very real problem of single-band transmission of communications signals.

Wide use, mainly in long-distance communications, has been made of the method of single-band transmissions via amplitude modulation, with subsequent filtering of one of the sidebands. In addition, in Soviet and foreign periodicals we find reports in which the problem of single-band communications is solved in other ways. In an article (Bibl.5) we find a method for optimum amplitude-phase modulation, while another article (Bibl.6) gives a method of two-phase modulation and still another article (Bibl.7) a method of three-phase modulation.

The peculiar feature of these methods lies in the fact that they all require that the spectrum of the signal to be transmitted contain no zero frequency or components close to it.

In the first of the enumerated methods, this requirement is correlated with the need to filter one of several closely adjacent modulation sidebands. All the other methods utilize broad-band phase converters. The demands made of these are very rigid since the effectiveness of suppressing the unnecessary sideband is determined by the accuracy of phase switching in all the components of the signal spectrum by one and the same angle. It was therefore not by chance that a series of articles appeared, discussing the theory and calculation of broad-band phase converters. These articles show that the technically attainable accuracy of phase switch is smaller, the larger the ratio of the highest frequency of the signal to the lowest frequency becomes. From this results the necessity for the above-formulated condition.

Thus, the use of the enumerated methods of single-band communications in a number of cases, e.g., in phototelegraphy, transmission of high-quality television programs, etc., is rendered difficult since the signal spectrum encompasses frequencies that are close to zero.

STAT

321

In accordance with the above statements it would also seem of interest to solve the problem of single-band communications so as to eliminate the above restriction. Since communications signals are signals with limited spectra, this solution might be found on the basis of some fundamental arguments in the theory of signals with limited spectra.

The theory of signals with limited spectra is based on the theorem by V.A. Kotelnikov, according to which every signal u(t) occupying a frequency band from 0 to ω_c can be expressed by the series:

$$u(t) = \sum_{-\infty}^{\infty} a_n \frac{\sin(\omega_c t - n\pi)}{\omega_c t - n\pi}. \qquad (10)$$

where $a_n = U\left(\frac{n\pi}{\omega_c}\right)$, n = 1, 2, 3,... .

The spectrum of this kind of signal, in the interval $-\omega_c < \omega < \omega_c$ can be presented as follows:

$$S(\omega) = \frac{1}{\omega_c}\sqrt{\frac{\pi}{2}}\sum_{-\infty}^{\infty} a_n e^{-in\pi\frac{\omega}{\omega_c}}. \qquad (11)$$

We will take as the initial signal to be converted for transmission in a single-band system a signal with a limited spectrum occupying the frequency band from zero to ω_c. The signal transmitted into the line in the single-band system we will consider as being obtained due to a displacement of the initial signal spectrum along the frequency scale by a magnitude Ω (Fig.4). The energy of this signal exists only in the frequency band from Ω to $\frac{\Omega}{\omega_c}$, which permits giving it the name "signal with band spectrum". Together with the idea of a signal with band spectrum, it is convenient to call the signal occupying the frequency band from zero to ω_c the "signal with a LF spectrum".

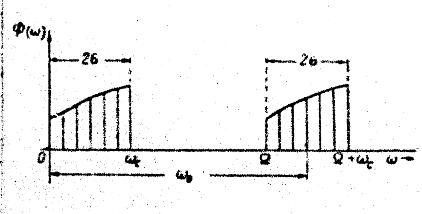

Fig.4

Giving the converted signal and its band spectrum the subscript 2, and utilizing eqs.(11) and (2), we get

$$S_2(\omega) = \frac{1}{\omega_c}\sqrt{\frac{\pi}{2}}\sum_{-\infty}^{\infty} a_n e^{in\pi\frac{\Omega-\omega}{\omega_c}}. \qquad (12)$$

Since

$$u_2(t) = \mathrm{Re}\,\frac{2}{\sqrt{2\pi}} \int_{\Omega}^{\Omega+\omega_c} S_2(\omega)\, e^{i\omega t}\, d\omega,$$

then, after integration

$$u_2(t) = \sum_{-\infty}^{\infty} a_n \frac{\cos \Omega t \cdot \sin(\omega_c t - n\pi) - \sin \Omega t\,[1 - \cos(\omega_c t - n\pi)]}{\omega_c t - n\pi}, \tag{13}$$

or

$$u_2(t) = \sum_{-\infty}^{\infty} a_n \frac{\sin\left(\sigma t - n\frac{\pi}{2}\right)\cdot\cos\left(\omega_0 t - n\frac{\pi}{2}\right)}{\sigma t - n\frac{\pi}{2}}, \tag{14}$$

where $2\sigma = \omega_c$ is the width of the signal spectrum;

$\omega_0 = \Omega + \frac{\omega_c}{2}$ is the central frequency of the signal spectrum.

Equations (13) and (14) represent, in a different form the breakdown of the signal $u_2(t)$ with a band spectrum through ordinates a_n of the initial signal with a LF spectrum*. They indicate the basic possibility of a direct synthesis of a signal with band spectrum in terms of the ordinates of the initial signal with a LF spectrum, in which no limitations are placed on the spectrum of the initial signal because of the zero and adjacent frequencies.

Appendix

A highly graphic representation for the shift of a spectrum is given by introducing the concept of a complex, or analytical, signal (2, 3, 4), defined in the following manner

$$\dot{F}(t) = \frac{2}{\sqrt{2\pi}} \int_0^{\infty} S(\omega)\, e^{i\omega t} d\omega. \tag{1.1}$$

To the complex function $\dot{F}(t)$ corresponds, in the plane of complex numbers, the radius-vector $\bar{F}(t)$ (Fig.5), rotating about the origin of the coordinates at the instantaneous velocity

$$\omega(t) = \frac{d}{dt} \arg \dot{F}(t). \tag{1.2}$$

In this definition of a complex signal, the projection of the vector $\bar{F}(t)$ onto

* The breakdown of a signal with a band spectrum is discussed in Bibl.8. In it, however, the signal with a band spectrum is approximated by the sum of two series whose ordinates serve as the coefficients of this same signal.

STAT

the real axis coincides with the real signal f(t) since by virtue of eq.(3) we have

$$f(t) = \mathrm{Re}\,[\dot F(t)].$$

On the basis of eqs.(1.2) and (1.3) we can introduce the concept of the instantaneous phase and instantaneous frequency of the real signal f(t), as magnitudes which coincide respectively with arg $\dot F(t)$ and $\omega(t)$. The bending frequency of the signal will be the modulus of the vector $\bar F(t)$. Thus,

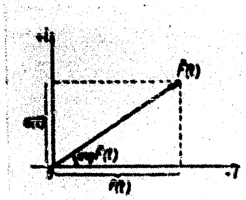

Fig.5

$$f(t) = |\dot F(t)|\cos[\arg \dot F(t)].$$

The projection of the vector $\bar F(t)$ onto the imaginary axis

$$\sigma(t) = \mathrm{Im}\,[\dot F(t)]$$

coincides with a quadrature signal all of whose spectral components are phase-shifted relative to the spectral components of the signal $\dot F(t)$ by an angle $\frac{\pi}{2}$. Equation (1.1) permits handling the complex signal $\dot F(t)$ as the infinite sum of infinitely small vectors:

$$d\dot F(t) = \frac{2}{\sqrt{2\pi}} S(\omega)\, e^{i\omega t}\, d\omega,$$

each of which rotates about the origin of the coordinates with constant angular velocity ω. A shift of the spectrum by a magnitude Ω corresponds to a change in the rotational velocity of each of the vector terms by Ω.

Let us suppose that the signal to be converted $f_1(t)$ corresponds to the complex signal $\dot F(t)$ and the converted signal $f_2(t)$ to the complex signal $\dot F_2(t)$. Then,

$$d\dot F_2(t) = e^{i\Omega t}\, d\dot F_1(t).$$

If upon displacement none of the elementary vectors dF(T) changes its direction of rotation, then:

$$\dot F_2(t) = e^{i\Omega t}\, \dot F_1(t). \qquad (1.4)$$

Equation (1.4) describes a spectrum shift up the frequency scale by any magnitude ($\Omega > 0$), and also down the frequency scale ($\Omega < 0$), where Ω, in absolute magnitude, does not exceed the lowest frequency in the spectrum of the signal to be converted. Thus, eq.(1.4) in a form different from the previous formulas (5) and (6), describes the reversible shift process. The process of spectrum shift is irreversible if the rotation direction of the elementary component parts of the complex signal changes to the opposite.

BIBLIOGRAPHY

1. Kharkevich,A.A. - Spectra and Analysis, GITTL (1953)
2. Gabor,D. - JIEE, Vo.93, Part III, Nov.1946.
3. Ville,J. - Cables & Transmission, No.1(1948)
4. Oswald,J. - Cables & Transmission, No.3 (1950)
5. Tetelbaum,S.I. - A Method of Raising the Effectiveness of Radio Communication, ZhTF, No.17 (1939)
6. Norgaard - QST, VI (1948)
7. Stein,B.B. and Varganov,G.G. - Separation of One Sideband by Multiphase Modulation. Nauchno-Tekhnichesky Sbornik MEIS (1950)
8. Weaver - PIRE, No.4 (1954)
9. Kohlenberg - J. of Appl. Phys., Vol.24, No.12 (1953)

Received by the Editors on 13 September 1955.

STAT

LETTERS TO THE EDITOR

Dear Editor:

The workers at the Kiev television center have successfully devoted themselves to increasing the definition of the television picture at the output of the video transmitter.

After carrying out the necessary work in expanding the frequency band of the video transmitter, the clarity of the picture in the horizontal was raised to 600 lines on the main feeder, this making it entirely possible to realize full quality of the image furnished by the studio equipment. This significantly surpasses the technical ratings for the television transmitter used in the Kiev television center.

We ask you to publish in your journal the enclosed letter since, in our opinion, the results we obtained might be of use to other centers using transmitters of the same type (Moscow, Leningrad, etc.).

In Soviet television centers we use two types of video transmitters: one with modulation on the final-stage tube grids (transmitters in the Leningrad, Moscow and Kiev television centers) and one with modulation in one of the intermediate stages (standard television-radio station).

One of the basic demands made of any television transmitter is that it realize to the greatest degree possible the quality factors of the television picture supplied by the studio equipment, in particular the sharpness.

In the circuits of second-type transmitters, this problem is solved with comparative ease since here it is possible, by tuning several circuit systems, to obtain a rather wide frequency characteristic for the UHF channel.

In transmitters of the first type, which have only one pair of circuits (in the final modulated stage) the possibilities of expanding the pass-band of this stage are greatly limited, so that the sharpness of the transmitted picture is also limited.

In terms of factory ratings, this band equals about 4.5 mc, which makes it possible to transmit 450-470 lines in terms of the horizontal key of the test table 0249.

Nevertheless, as the research described below has shown, even in this case the sharpness can be considerably increased. To solve this problem, the Kiev television center decided on a method of mutual compensation of the frequency characteristics of the modulating device and the modulated stage. It was necessary to create some rise in the frequency characteristic of the modulator at the upper modulating frequencies (4-6 mc) in order to compensate the drop in frequency characteristic of the modulated stage at these same frequencies. The system of two coupled circuits, used in the final modulated stage, has a frequency characteristic in the form of a shallow resonance curve with very smooth slopes, which permits the use of the above method.

We began our work on expanding and correcting the frequency characteristic of the modulation stage in the video transmitter by measuring the frequency characteristics of all the modulator stages. These measurements showed that the first two stages alone narrow the frequency band by more than 1.7 mc (cf. broken curve in Fig.1)*.

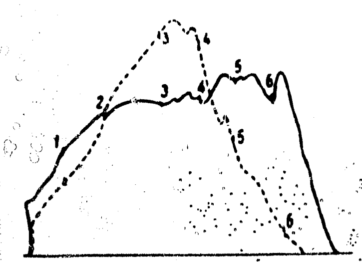

Fig.1

Taking into account that, to transmit 600 lines in the horizontal, we need a frequency band of the order of 6.3-6.5 mc, we first had to correct these two stages.

Since we had to conduct all our experiments without interfering with normal operation, we did not reconstruct the working equipment, but worked on specially de-

* All measurements were made with an IChKh-1 instrument. The numbers designate frequency in megacycles.

signed first and second stages which served simultaneously as reserve equipment. They were constructed basically according to the circuit diagram of the existing equipment and contained the same tube, but the inductance of the coils of grid and plate correction was increased so as to broaden the adjustment limits. The use of these stages, despite a large number of experiments, permitted no noticeable expansion in their pass-band. This was explained by the small amplification factors of the 6P13 tubes used in the first stage. We therefore replaced the five parallel-connected 6P13 tubes in the first stage by five 6P19 tubes. The amplification of this stage rose more than 2.5 times:

$$kf_{v} = \frac{S}{2\pi C} = \begin{cases} 25 \ldots \text{for the Tube 6P3} \\ 58.5 \ldots \text{" " 6P9} \end{cases}$$

Specifically, the amplification factor at a frequency of 6.5 mc rose to 9 when using 6P19 pentodes, instead of 3.5 in the 6P13 tubes.

After replacing the tubes we tuned these two stages and checked the amplitude characteristic of the AC amplifiers (the first four stages of the modulator). Here we found that

1) the amplitude characteristic remained linear within the limits of 6   at the input of the first stage, which considerably exceeded the maximum operating scope of the 5-volt signal;

2) the pass-band of these two stages expanded by 1.7-1.8 mc (cf. continuous curve in Fig.1).

The measurements were conducted on the tube grids of the third stage of the modulator.

After correcting the frequency characteristic of the first two stages, we proceeded to partial tuning of the third stage and to a considerable tuning of the fourth and fifth stages of the modulators so as to expand their pass-bands and also to create a rise in frequencies from 4 to 6.5 mc. This tuning was done only by means of elements in the complex correction circuits existing in the three above stages, without changing the circuits of the stages themselves.

STAT

The most noticeable influence on the slope of the frequency characteristic, as we found in the given case, is produced by the grid inductors; the most advantageous (from the point of view of the entire modulator characteristic) number of turns was selected experimentally. In addition, some improvement in the pass-band was obtained by means of plate inductors.

Obtaining a rise of 4-6 mc in frequency represents a rather complicated problem since extreme care must be taken in selecting the number of turns in the correction coils of the various stages, and accordingly a great many measurements must be made. In this case, one or two turns are required.

As a result of all our work we were able to obtain a frequency characteristic for the entire modulator in the form of the curve shown in Fig.2 as a continuous line. Here, for comparison, we also show the modulator characteristic before tuning.

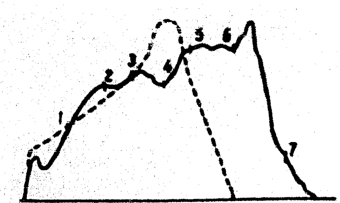

Fig.2

Our observations were conducted directly on the tube grids of the modulated stage. Figure 2 shows that the pass-band of the modulator was enlarged by 1.7-1.8 mc and a considerable rise was realized at frequencies of 4-6.5 mc.

After correcting the video-control devices to have their amplifiers pass through a uniform frequency band up to 6.5 mc, we measured the sharpness of the picture in accordance with the test table 0249. As our measurements on the main feeder showed, the sharpness in the vertical and the group definition was equal to 600 lines (with the same sharpness at the modulator input). The remaining quality specifications did not degenerate at all in this process.

The above method for raising the sharpness indexes by an artificial rise in the frequency characteristic of the modulator in video-transmitters with modulation in the final stage can obviously be applied to non standard transmitters as well, both

321

those under construction and those in actual use.

Senior Engineer of UHF Radio Station, Y. Omelyanenko.

6 January 1956.

Magnetic Microphone with Semiconductor Amplifier

The Remler Co. (USA) has put out a magnetic microphone with a built-in amplifier. The vibrations of a membrane made of beryllium copper are transmitted to the magnetic system by a stainless steel pin. The additional amplification due to the low output volume of the microphone is accomplished by using a two-stage amplifier, working on semiconductor triodes. The microphone and amplifier together occupy as much space as is required by an ordinary microphone.

The amplifier works under limiting conditions so as to ensure constant volume for different distances between the speaker and microphone. The new microphone has the same output resistance and volume as the ordinary carbon microphone, so that it can be substituted for the latter. The amplifier is enclosed in a plastic casing impermeable to air and water.

Technical specifications of microphone and amplifier:

Output voltage: 0.778 v eff.
for 100 bar.

Input resistance: 150 ohms

Feed voltage: 27.5 volts

Frequency response: ± 6 db in the frequency band 500-6000 cps,
below 500 cps blocking of 6 db.

Ambient temperature: +50°C maximum.

A drop in feed voltage from 27.5 v to 15 v causes the output volume to drop by 2 db.

The above specifications are valid for a temperature range from -50 to +50°C, at a relative humidity of 95-100% and at altitudes up to 15,000 m.

The microphone is not sensitive to periodic jarring or to dropping.

STAT

In the USA, the new microphone is widely used in aviation for air-to-ground communication and operates reliably for a long period of time.

A Silicon Rectifier

The laboratories of the Bell Telephone Co. (USA) have developed a silicon rectifier the size of a pea, which can be used for feeding telephone stations with rectified current. According to company representatives, the rectifier is superior to all previous dry rectifiers, has an almost limitless service time, and can work for a long time at high efficiency under temperatures as high as +200°C.

Two such rectifiers, provided with special casings to improve the heat dissipation, yield rectified current up to 20 amp at a voltage of 100 v, i.e., a power of 2 kw. The total heat losses equal 20 w.

To produce these rectifiers, almost pure silicon (less than one atom of impurities per billion atoms of silicon) is required. After purifying the silicon it is mixed with small, accurately controlled amounts of additives by treating the silicon with vapors at high temperature. As a result, silicon with conductivity of the p-n type is obtained, used also in producing semiconductor triodes.

The cost of the silicon is very high, but only small amounts are needed. The pea-size rectifier has a strip of silicon 2.5 mm long and 0.127 mm thick.

For electronic computers small rectifiers are produced by this firm. Where high-power rectified current is needed, the dimensions of the silicon strip and the thickness of the lead-outs are increased.

NEW BOOKS

Radio Engineering and Electronics, their Technical Application. Edited by A.I.Berg and I.S.Dzhigit. Izd. AN SSSR, 1956, 128 pages, 25,000 copies, 1 ruble, 90 kopeks.

This pamphlet prepared for the 20th Congress of the CPSU under the general supervision and with the direct cooperation of several members of the Radio Soviet under the presidium of the AN SSSR, gives a popular description of radio engineering and electronics and of the application of their methods in radio electronics, radio communications, radio broadcasting, radar and radio navigation, and of the use of radio electronics in science, technology, and industry.

Radio Relay Communications Lines. Collection of articles, edited by V.A.Smirnov. Izd. Inostrannoi Literatury, 1956, 584 pages, 25 r, 85 k. bound.

This collection gives translations of 27 articles published in foreign journals and dealing with theoretical problems and methods in the calculation of radio relay lines, practical problems in planning lines and equipment, including a description of the TD-2 system for transmitting six broad-band trunks in one direction.

A.D.Fox, S.E.Miller, and M.T.Weiss. Properties of Ferrites and their Use in the UHF Range. Translation from English by L.G.Lomize. Edited by R.G.Mirimanova. Izd. "Sovyetskoye Radio", 1956, 99 pages, 4 r. 10 k.

The pamphlet discusses the passage of electromagnetic waves through gyromagnetic media in the presence of a longitudinal or transverse external magnetic field; it handles problems involved in creating wave-guide systems with valve properties and describes a gyrator, isolator and circulator realized by means of rotating a polarization plane and by means of other effects inherent to ferrites.

G.Soul and L.Walker. Wave-Guide Propagation of Electromagnetic Waves in Gyrotropic Media. Translation from English by L.G.Lomize, Y.A.Monosov and V.E.Kostyleva.

STAT

330

Edited by R.G.Mirimanov. Izd. Inostrannoi Literatury, 1955, 189 pages, 7 r. 35 k.

This monograph discusses a cylindrical wave-guide with total packing, and also transverse magnetisation, irreversible spirals, and the application of methods from the theory of perturbations to the study of some supplementary problems.

S.Shchelkunov and G.Frins. Antennas, Theory and Practice. Translation from English, edited by L.D.Bakhrakh. Izd. "Sovyetskoye Radio", 1955, 604 pages, 28 r. 35 k. bound.

The book discusses subjects in the theory, calculation, and design both of radio broadcasting and communications antennas, as well as antenna arrays in the centimeter range.

G.P.Shkurin. Handbook of Electric and Radio Measuring Instruments. 2nd Edition, revised and enlarged. Voyenizdat, 1955, 912 pages, 19 r. 15k. bound.

The first part of the handbook describes 192 different types of electric measuring instruments. The second part describes 40 types of radio measuring instruments. In describing the instruments, the author gives brief information on the purpose, field of use, specifications, and construction of the instrument, and also indicates under what GOST or technical conditions it was produced. For radio measuring instruments, the basic diagrams and specifications of the units in the diagram are given.

Appendices to the book give a price list grouping the instruments according to their type and purposes. Their measuring limits and degree of accuracy are indicated.

ACCEPTANCE FOR GRADUATE WORK

The Central Scientific Research Institute of Communications of the Ministry USSR (TsNIIS) announces openings for graduate work for 1956 in the following specialties:

1. Long-distance communications.
2. Telegraph communications.
3. Linear-cable communications equipment.
4. Communications economics.

Eligible for graduate work scholarships are persons with higher degrees, maximum age 40 years, having industrial experience of no less than three years in the particular specialty.

The application for graduate study must be accompanied by

a) a notarized copy of diploma (2 copies)

b) list of previous employment (2 copies)

c) biographical sketch (2 copies)

d) document on military status (1 copy)

e) political and work record from last place of employment (2 copies)

f) health certificate (1 copy)

g) list of scientific works and inventions (2 copies)

h) paper on some theme in the selected specialty (1 copy)

i) two small photographs.

Applications will be accepted until August 15.

Entrance tests at the level of higher schools on Marxism-Leninism, on a discipline from the chosen specialty and on one foreign language will be given from October 1 to 20.

Persons accepted for the entrance tests will be given one month leave with pay from their place of employment to prepare for the tests in accordance with article 13 of the "Statutes for Graduate Study" ratified by the Soviet of Ministers USSR, in decree No.4655, dated 11/17/50. The document authorizing absence from work is the Institute's admission paper to the entrance examinations.

Persons accepted for graduate study after the examinations are freed from employment under paragraph 14 of the "Statutes for Graduate Study" and are bound to appear at the Institute by the beginning of the academic term. The credentials for release from employment for persons accepted for graduate work is the notice sent by the Institute. Single, out-of-town students are guaranteed dormitory quarters.

Applications and requests for information should be addressed to: Moskva, E-43, Pervaya Parkovaya ul., 7/a, TSNIIS, tel. E 5-30-55; E 5-00-11, dob. 2-13.